THE MEAN VELOCITY DISTRIBUTION IN FULLY DEVELOPED TURBULENT WATER FLOW IN A STRAIGHT CIRCULAR PIPE

By

DONALD FRANK HABER

Bachelor of Science
University of Missouri at Rolla
Rolla, Missouri
1956

Master of Science
University of Missouri at Rolla
Rolla, Missouri
1962

Submitted to the Faculty of the Graduate
School of the Oklahoma State University
in partial fulfillment for the requirements
for the degree of
DOCTOR OF PHILOSOPHY
May, 1966

OKLAHOMA
STATE UNIVERSITY
LIBRARY
NOV 8 1966

THE MEAN VELOCITY DISTRIBUTION IN FULLY DEVELOPED TURBULENT WATER FLOW IN A STRAIGHT CIRCULAR PIPE

Thesis Approved:

Quintin B. Graves
Thesis Adviser

James A. Clark

Robert L. Jones

Paul G. McCollum

J. H. Boggs
Dean of the Graduate School

621546

ACKNOWLEDGMENT

Indebtedness and sincere appreciation is extended to the following individuals and organizations:

Professor J. L. Chao, who served as my thesis adviser. His keen knowledge of experimental techniques greatly helped me during the tedious hours spent improving the system.

My graduate committee, composed of Professors Quinton B. Graves, who served as my committee chairman, R. L. Janes and P. L. McCollum for their advice and encouragement.

Professor E. R. Lindgren, who first presented the problem and encouraged research in this area.

The Office of Naval Research for financial support of the research.

The Ford Foundation and the College of Engineering of Oklahoma State University for financial support throughout my graduate study.

Mr. Cecil Sharpe, Mr. Preston Wilson, and Mr. Arlin Harris, who helped build and modify the experimental system.

Mrs. Peggy Harrison for her expert typing of this thesis.

My wife Edith and children Kristin, Daniel, and Kimberly for their sacrifices. Especially my wife who provided encouragement, optimism and solace during the many periods of difficulty.

D. F. H.

January 14, 1966
Stillwater, Oklahoma

TABLE OF CONTENTS

LIST OF FIGURES

NOMENCLATURE

Symbols defined here are the ones used through out the text.

x, y, and θ. .	Cylindrical coordinates;
u	Mean velocity component in x direction;
U_{max}	Maximum velocity component in x direction;
$\overline{U}$	Average velocity (flow rate/cross-sectional curve);
u', v', w' . . .	Fluctuating velocity components in the x, y, and θ directions, respectively;
D	Inside diameter of test pipe;
R	Inside radius of test pipe;
μ	Dynamic viscosity
ν	Kinematic viscosity;
ρ	Mass density;
Re	Reynold's number $(\frac{\overline{U}\,2R}{\nu})$;
x	Universal constant (usually taken as 0.4);
Q	Flow rate;
τ_w	Wall shear stress;
u^*	Frictional velocity $(\sqrt{\frac{\tau_w}{\rho}})$;
t	Time.

CHAPTER I

STATEMENT OF THE PROBLEM

The concept of a thin layer of fluid in which viscous shear stresses are very much greater than turbulent shear stresses and which is adjacent to the bounding wall of a pipe containing fully developed turbulent flow was first experimentally investigated by Stanton, Marshall and Bryan in 1920 (1). The results of the investigation did not prove such a sublayer existed because of the difficulties the investigators experienced in the measurement of velocities close to the bounding wall. However, the experimental results did seem to indicate a region of fluid adjacent to the pipe wall in which the mean velocity varied linearly with distance from the wall (this showed a predominance of viscous shear stress).

In 1930, Nikuradse (2) published the results of his classic work on the mean velocity distribution of water in turbulent pipe flow. These results differed from those of Stanton, Marshall, and Bryan in that the velocity distribution did not vary linearly with distance from the pipe wall in a fluid layer close to the wall. In fact, Nikuradse's results seemed to predict a finite velocity existing at the pipe wall (slip occurring between the water in contact with the wall and the wall itself). Figure 1 illustrates Nikuradse's 1930 results. Nikuradse used two dimensionless variables $\frac{u}{u^*}$ and $\frac{yu^*}{\nu}$ (where $u^* = \sqrt{\frac{\tau_W}{\rho}}$) to report his results.

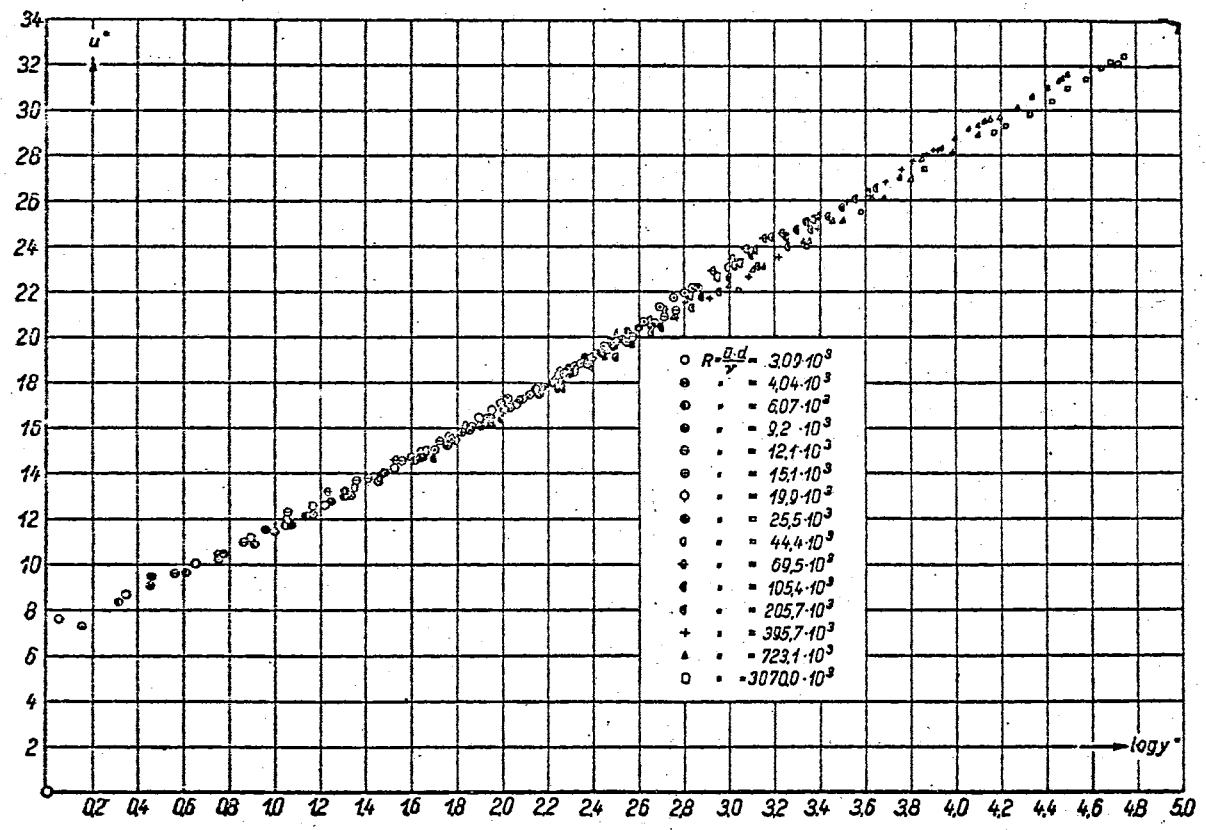

Abb. 15. u^* in Abhängigkeit von $\log y^*$.

Figure 1

Nikuradse's 1930 Experimental Results (Taken from "Widerstandsgetz und Geschwindigkeit-verteilung von Turbulenten Wasserstramungen in glatten and rauhen Rohren." Proc. 3rd ICAM, Vol. 1, p. 239, Stockholm, 1930.)

In general, these results show a logarithmic relationship between two variables throughout the entire pipe cross-section.

In 1932, Nikuradse (3) published the same experimental results a second time. The 1932 results, however, differed significantly from his 1930 results in the plotted values for velocities near the pipe wall. The 1932 results agreed with the viscous sublayer hypothesis and furthermore gave no indication of a finite velocity at the wall. Figure 2 shows the difference between the two reported results.

Miller (4) carefully analyzed Nikuradse's 1932 report and found a discrepancy between the tabulated values of the mean velocity and the points plotted on the dimensionless velocity profile. Miller could not find a valid reason for the difference between the plotted and tabulated values of mean velocity and instigated an investigation of the discrepancy. The outcome of Miller's investigation showed that Nikuradse had apparently shifted some experimental points to force his experimental values to agree with the viscous sublayer hypothesis.

Nikuradse, however, did not state that his work proved the existence of a viscous sublayer. But subsequent writers on fluid mechanics use Nikuradse's changed results as proof of the existence of such a sublayer.

Since Nikuradse's work in 1930 did not attempt to explore thoroughly the region adjacent to the pipe wall, Reichard (5) undertook an investigation of the mean velocity in this region. He used the technique of hot-wire anemometry along with fine pitot tubes to

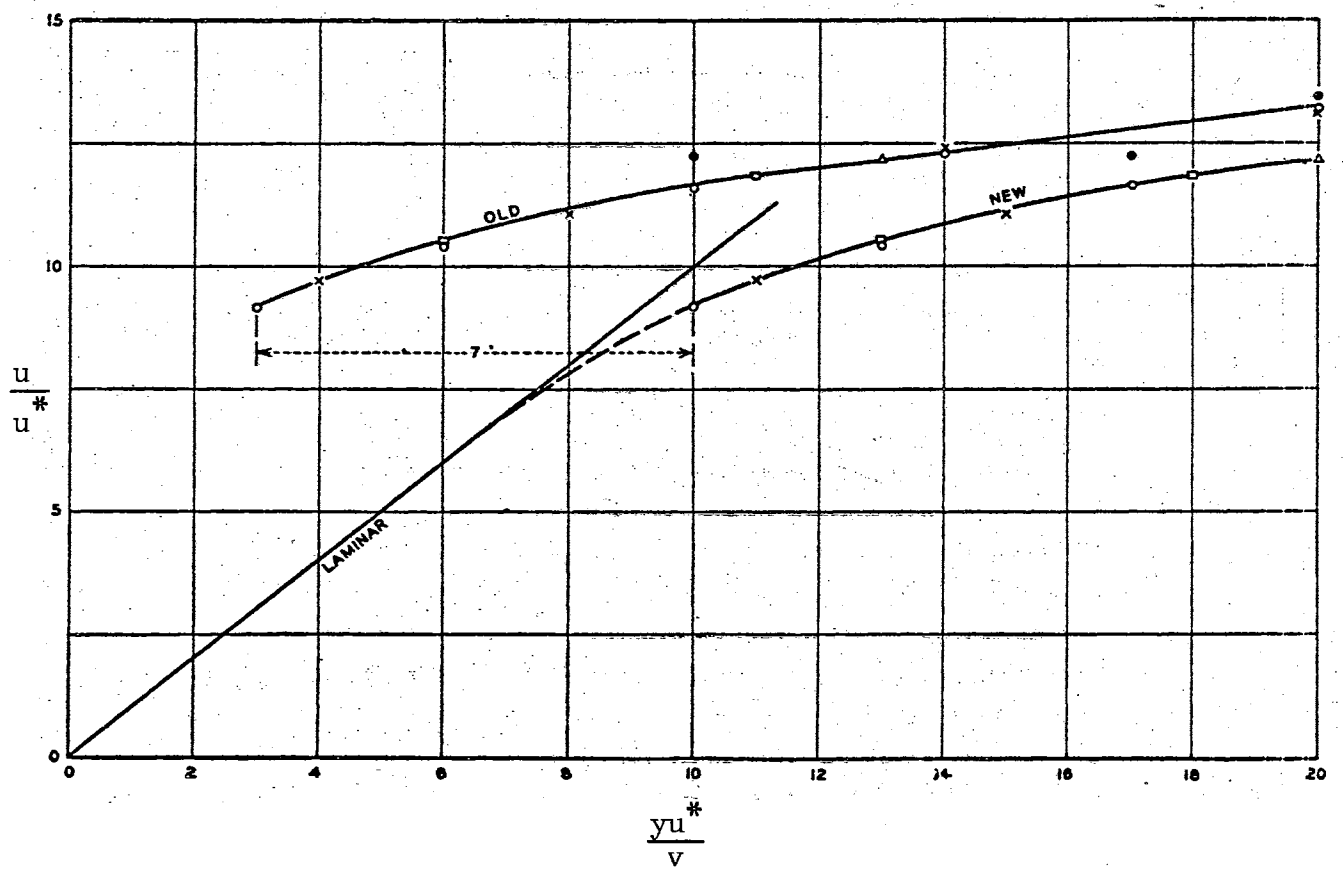

Figure 2

An illustration of the shift of experimental results from Nikuradse's 1930 report to the 1932 report. (Taken from "Laminar Film Hypothesis" by Miller, Trans. ASME, Vol. 71, May 1949, p. 364.)

measure the mean velocity distribution of air in a rectangular channel. His results indicate a deviation from the logarithmic relationship near the wall. They also seemed to agree with the laminar hypothesis.

Reichardt, however, experienced difficulties in measuring low velocities near the bounding wall, because the low velocities were easily disturbed by external causes. For instance, small temperature differences between the air stream and the wall caused observable changes in the velocity distribution. Therefore, his velocity profile was almost always slightly unsymmetrical and u^* was different on the upper and lower walls of the channel. Reichardt's measurement of pressure drop along the channel gave results for u^* which did not agree with those of other investigators. He, therefore, corrected his $\frac{u}{u^*}$ values to agree with Nikuradse's.

Laufer (6), in 1954, reported results of a very carefully conducted experimental investigation of the structure of shear flow in straight circular pipes, including measurements of the mean velocity distribution across the pipe cross-section. He used a 10 inch I. D. smooth-walled brass pipe in which pitot tubes and hot-wire probes were used to measure the turbulent properties of air flow at maximum speeds of 10 ft/sec. and 100 ft/sec. In his mean velocity measurements near the wall (the closest .001 inches away), a correction had to be made because of the large velocity fluctuations for both the pitot tube and the hot-wire probes. He does not mention any wall interference for either the hot-wire or the pitot tube measurements, although he states that the hot-wire results were unreasonably low in the vicinity of the wall.

The results of this investigation indicated a region adjacent to the wall following the laminar sublayer hypothesis. However, Laufer found that the velocity fluctuations u', v' and w' from the mean velocity were present even within the viscous sublayer. This indicated that the flow in the wall region is not a truly laminar flow. The mean velocity results, outside the sublayer, followed the logarithmic relationship between $\frac{u}{u^*}$ and $\frac{yu^*}{\nu}$, as reported by Nikuradse, but with slightly different constants. The logarithmic relationship did not carry through the entire pipe cross-section as did Nikuradse's, but deviated from the logarithmic near the center of the pipe.

Laufer's results did indicate very good agreement between the mean velocity gradient calculated from pressure drop measurements and the velocity gradient found directly from the measured velocities. Although the pressure drop — velocity gradient measurements were in agreement, other investigators, namely Schubauer in 1934 (7), Dryden in 1936 (8), and Abbrect and Churchill (9), experienced very definite wall measuring effects when using a hot-wire probe close to a solid boundary. Since Laufer's measurements were within .001 inches of the boundary, a wall effect on the hot-wire probe should have been noticed which could account for his "unreasonably low values" near the pipe wall.

There are other works in which the question of the mean velocity distribution in turbulent pipe flow was investigated, however, none of them are nearly as detailed or complete as Laufer's. All investigators who have had their results published (within the author's knowledge) have used air as the fluid medium, with the exception of

Nikuradse. Pitot tubes and hot-wire probes were used as the velocity measuring devices. Most of these investigators, Nunner (10), Deissler (11), Rothfus, Monrad and Senecal (12), and Abbrect and Churchill (9), were mainly concerned with the logarithmic region outside the sublayer. However, if the investigation was carried on near the wall, elaborate corrections for pitot tube measurements were devised or no corrections were used and the question of wall effects was carefully avoided.

Coles (13) sums up the question of the laminar or viscous sublayer as follows: "Within the sublayer, large fluctuations in velocity and cramped quarters for experimentation usually combine to make measurements of mean velocity somewhat uncertain. The available data, therefore, should not be said to establish conclusively the uniqueness of the 'Law of the Wall' in the sublayer."

The main purposes of this investigation are: 1) to resolve the contradiction in Nikuradse's work, especially concerning the region adjacent to the wall by using water as the fluid medium; 2) to attempt to establish the validity of the "Law of the Wall" in the sublayer region for the turbulent flow of water in circular pipes; 3) to investigate the "Law of the Wall" relationship outside the viscous sublayer including the core region of turbulent pipe flow.

CHAPTER II

ANALYTIC BACKGROUND ON THE MEAN VELOCITY DISTRIBUTION IN FULLY DEVELOPED TURBULENT PIPE FLOW

2.1. Introduction

The most recent hypothesis concerning the mean velocity distribution in turbulent smooth pipe flow can be found summarized in reports by Clauser (14), Hinze (15), and Coles (13). The hypothesis is based upon the experimental evidence reported by investigators into the boundary layer along a smooth flat plate (see Clauser pp. 6-7 (14)) and the mean-velocity distribution in turbulent pipe flow. (See Chapter I). This hypothesis assumes that for an adequate description of mean velocity distribution in both turbulent pipe flow and turbulent boundary layers along flat plates, two distinct regions must be identified. These are: An inner or wall region and an outer or core region. Each region is characterized by essentially different flow phenomena.

2.2. Inner Region

The mean velocity distribution in the inner region is assumed to depend on four variables, that is Eq. 2-2.1

$$u = f(y, \rho, \mu, \tau_w) \qquad (2\text{-}2.1)$$

Two independent dimensionless groups can be formed from these variables and expressed as

$$\frac{u}{u^*} = f\left(\frac{yu^*}{\nu}\right) . \qquad (2\text{-}2.2)$$

This relationship is known as the "Law of the Wall". However, within the inner region itself another division can be made. For the case of a smooth wall boundary, in a thin layer adjacent to the wall the flow is thought to be dominated by viscous stresses (this region was called the viscous sublayer in Chapter I). If the no slip assumption is made, the variable $\frac{u}{u^*}$ approaches $\frac{yu^*}{\nu}$ as y approaches zero and the "Law of the Wall" can be reduced to the following form

$$\frac{u}{u^*} = \frac{yu^*}{\nu} . \qquad (2\text{-}2.3)$$

That is, considering fully developed turbulent pipe flow, the total shear stress at any point is given by

$$\tau = \mu \frac{\partial u}{\partial y} - \rho \overline{u'v'} .$$

In the viscous sublayer, however, the turbulent shear stress $\rho \overline{u'v'}$ is assumed negligible compared with the viscous stress $\mu \frac{\partial u}{\partial y}$ and

$$\tau = \mu \frac{\partial u}{\partial y} .$$

At the wall itself,

$$\tau = \tau_w = \mu \frac{\partial u}{\partial y} .$$

Assuming the shear stress τ is constant in the thin viscous sublayer and equal to τ_w

$$\frac{\tau_w}{\mu} = \frac{\partial u}{\partial y} \quad \text{where} \quad \mu = \rho v ,$$

and

$$\frac{\tau_w}{\rho} = \nu \frac{\partial u}{\partial y}$$

finally

$$u^{*2} = \nu \frac{\partial u}{\partial y} .$$

Integrating $u^{*2} = \nu \frac{\partial u}{\partial y}$.

$$u^{*2} y = \nu u + c \qquad \text{(but at } y = 0,\ u = 0 \text{ (no slip), therefore } c = 0\text{)}$$

and the following equation

$$\frac{u^* y}{\nu} = \frac{u}{u^*} \qquad \text{results.}$$

This is exactly the same as Eq. 2-2.3 presented earlier. As pointed out in Chapter I, most of the experimental evidence reported seems to support this form of the "Law of the Wall" in the viscous sublayer the although Nikuradse's 1930 experimental results are a notable exception.

Outside the sublayer, in the other part of the inner region, fully developed turbulent flow is assumed to exist. The magnitude of the turbulent shear stresses are dominant, but the viscous stresses cannot be assumed negligible. This part of the inner region is still very near the bounding wall. For example, Hinze pp. 516 (15) on the basis of a summary of experimental evidence, approximates the distance of this

region from the wall by $\frac{u^* y}{\nu} = 30$. Using Blasius' formula for frictional resistance of smooth pipes (an empirical relationship experimentally shown valid up to Re = 100,000), and for turbulent flow in a pipe with Re = 5000, the distance to fully developed turbulent flow can be found. That is, with Blasius' formula

$$u^* = (0.3325)^{1/2} \frac{\bar{u}^{7/8} \nu^{1/8}}{Re^{1/8}} .$$

Since

$$\frac{u^* y}{\nu} = 30$$

and

$$Re = \frac{\bar{u} D}{\nu} = 5000$$

Then

$$\frac{y}{D} = 0.09.$$

Because this inner region is relatively close to the wall, the flow is still thought to be influenced by wall shear and the fluid viscosity. Prandl (16), based upon his mixing length theory and the experimental evidence of Nikuradse, predicted that the "Law of the Wall" in this inner region would have the form

$$\frac{u}{u^*} = A \log \frac{y u^*}{\nu} + B , \qquad (2\text{-}2.4)$$

where A and B are constants.

This logarithmic region along with the viscous sublayer is also characterized by its relative independence from disturbances from the outer or core region whether the flow in the core region occurs in a boundary layer or in a pipe or channel. Clauser, p. 17 (14) has shown that disturbances in the inner region disappear much faster than the same type of disturbances in the outer region. Also, Clauser, p. 7 (14), Coles, p. 192 (12), Hinze, p. 479 (15), and others report excellent agreement of boundary layer experimental results with pipe and channel results for the mean velocity distribution in the inner region.

Between the logarithmic region and the viscous sublayer a transition zone is assumed to exist. That is a zone where the viscous stresses and the turbulent stresses have approximately the same magnitude. The "Law of the Wall"

$$\frac{u}{u^*} = f\left(\frac{yu^*}{\nu}\right)$$

is still assumed valid, although the exact form of the function has not been agreed upon. Hinze pp. 471-473 (15), summarizes the various proposed functional forms for the "Law of the Wall" in this region.

2.3. Outer Region

In 1932, Von Karman presented an empirical relationship, named the "Velocity-Defect Law", for the mean velocity distribution in turbulent pipe flow based on experimental evidence by Fritsch (16),

$$\frac{u_{max} - u}{u^*} = F\left(\frac{y}{r}\right). \qquad (2\text{-}3.1)$$

Although Von Karman first presented Eq. 2-3.1 in this general form, Stanton, Marshall and Bryan (1) in 1920 and Darcy also suggested using specialized forms of the velocity defect law to predict mean velocity distributions in turbulent pipe flow.

Clauser, p. 5 (14), showed that using the velocity defect relationship, a universal plot of turbulent boundary layer profiles could be obtained that was valid for all but the regions near the wall. Clauser also postulated a relationship for the entire velocity profile in the form

$$\frac{u}{u^*} = F_1\left(\frac{yu^*}{\nu}\right) + G_1\left(\frac{y}{r}\right) , \qquad (2\text{-}3.2)$$

where $F_1\left(\frac{yu^*}{\nu}\right)$ represents the logarithmic portion of the mean velocity distribution Eq. 2-2.4, and $G_1\left(\frac{y}{r}\right)$ the deviation of the mean velocity profile from the logarithmic line.

Millikan (18) in 1938, proved that there must be a logarithmic region for the mean velocity distribution, provided that the "Law of the Wall" and the "Velocity-Defect Law" are both valid in the same region.

If this equation

$$\frac{u}{u^*} = f\left(\frac{yu^*}{\nu}\right) \qquad (2\text{-}3.3)$$

is valid in a region where

$$\frac{u_{max} - u}{u^*} = F\left(\frac{y}{r}\right) \qquad (2\text{-}3.4)$$

is also valid, then differentiating Eq. 2-3.3

$$\frac{\partial u}{\partial y}\frac{1}{u^*} = \frac{u^*}{\nu} f'\left(\frac{yu^*}{\nu}\right)$$

and (2-3.5)

$$\frac{\partial u}{\partial y}\frac{y}{u^*} = \frac{u^*}{\nu} y f'\left(\frac{yu^*}{\nu}\right) .$$

Differentiating Eq. 2-3.4,

$$-\frac{\partial u}{\partial y}\frac{1}{u^*} = \frac{1}{r} F'\left(\frac{y}{r}\right)$$

and (2-3.6)

$$\frac{\partial u}{\partial y}\frac{y}{u^*} = -\frac{y}{r} F'\left(\frac{y}{r}\right) .$$

But Eq. 2-3.3 equals Eq. 2-3.4, then

$$-\frac{y}{r} F'\left(\frac{y}{r}\right) = \frac{u^* y}{\nu} f'\left(\frac{yu^*}{\nu}\right) = \frac{\partial u}{\partial y}\frac{y}{u^*} .$$

$\left(\frac{y}{r}\right)$ is completely independent from $\frac{yu^*}{\nu}$, therefore,

$$\frac{u^* y}{\nu} f'\left(\frac{yu^*}{\nu}\right) = \frac{1}{x}$$

(where x is a constant). Integrating over the region in question,

$$f\left(\frac{yu^*}{\nu}\right) = \frac{1}{x}\log\frac{yu^*}{\nu} + c . \qquad (2\text{-}3.7)$$

Now Eq. 2-3.5 can be compared to Eq. 2-2.4 and is exactly the same, if constants A and B are changed to $\frac{1}{x}$ and C respectively.

Coles (13), in 1956, extended the "Velocity-Defect Law" by proposing another universal function $w\left(\frac{y}{r}\right)$, which he named the "Law of

the Wake". Specifically, Coles proposed

$$\frac{u}{u^*} = f\left(\frac{yu^*}{\nu}\right) + \frac{\pi}{x}\, w\left(\frac{y}{r}\right), \qquad (2\text{-}3.8)$$

where π is a constant for fully developed turbulent pipe flow.

Actually the "Law of the Wake" gives the deviation of the mean velocity profile from the logarithmic portion throughout the core region.

Coles verified the existence of the "Law of the Wake" by comparing numerous experimental data, both in boundary layer flow and in pipe flow.

CHAPTER III

EXPERIMENTAL EQUIPMENT AND ARRANGEMENT

3.1. Water Tunnel

A schematic diagram of the water tunnel is shown in Figure 3. Distilled water was pumped into storage tank A (a cylindrical fiberglass tank, 1.23 m high by 1 m diameter). The storage tank was connected to a plexiglas mixing tank B by a small p.v.c. pipe and ball valve. The mixing tank containing a stainless-steel cooling coil of a 250 W heat exchanger was placed directly above the suction side of a glass-walled centrifugal pump C which was driven by a variable speed belt drive powered by a 3 H.P. electric motor. The pump could supply a maximum flow rate of 200 gpm to the system. An outlet p.v.c. pipe was connected to the pressure side of the pump and terminated in a large steel tank D. The inside of the steel tank was fiberglassed to prevent corrosion. Between the filter tank D and the pump, a system of valves along the connecting pipe allowed the flow rate to be adjusted without changing the speed of the pump. A 127 mm dia., 23.6 m long plexiglas pipe made up of eleven matching sections was connected to the steel tank D by a cylindrical flange and large diameter plexiglas pipe (12 in. diameter and approximately 36 in. long). Next to the flange of the steel tank, a fiberglass wool type filter was placed which effectively filtered large particles from the distilled water entering the 23.6 m long test pipe.

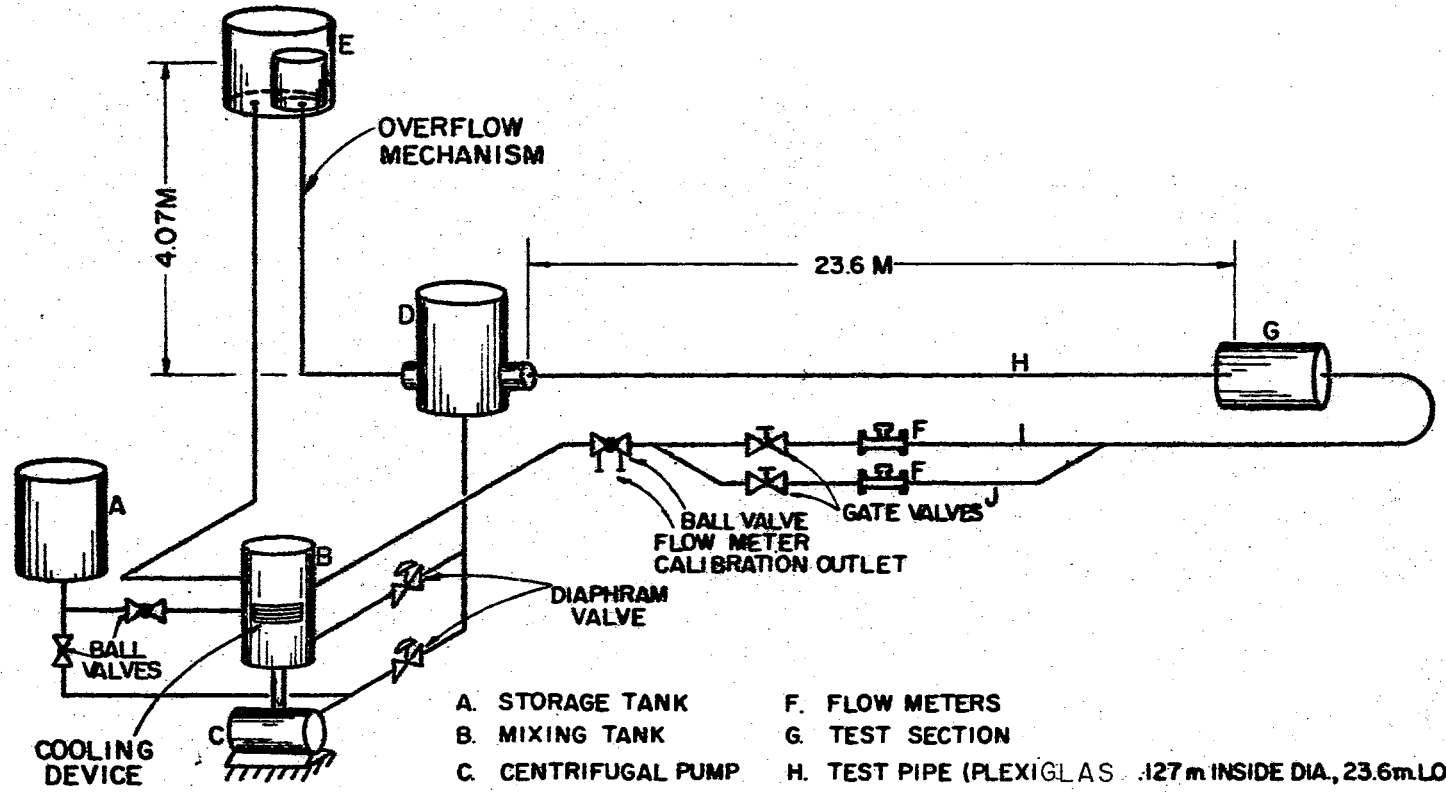
E
OVERFLOW
MECHANISM
4.07M
23.6 M
D
G
H
F
I
F
J
A
B
BALL VALVE
FLOW METER
CALIBRATION OUTLET
GATE VALVES
DIAPHRAM
VALVE
BALL
VALVES
COOLING
DEVICE
C
A. STORAGE TANK
B. MIXING TANK
C. CENTRIFUGAL PUMP
D. FILTER TANK
E. OVERFLOW TANK
F. FLOW METERS
G. TEST SECTION
H. TEST PIPE (PLEXIGLAS .127m INSIDE DIA., 23.6m LONG)
I. RETURN PIPE (PLEXIGLAS .076m. INSIDE DIA.)
J. RETURN PIPE (PLEXIGLAS .025m. INSIDE DIA.)

Figure 3

In the entrance region of the large diameter pipe a disturbance plate could be placed to develop fully turbulent flow rapidly. Also connected to the steel tank D was a constant pressure head arrangement (diagrammed in Figure 3). By keeping a small overflow into tank E, the pressure at tank D was kept constant. Thus the flow through test pipe H was maintained at an extremely constant value (within the accuracy of the flow rate measuring devices). The 23.6 m plexiglas pipe H was carefully straightened and leveled by a transit and level. The inside diameter of the test pipe was checked and found to vary less than .5 mm over its length. The ratio of the length of the test pipe H to the inside diameter of the test pipe was 186.

The test pipe H was inserted into a 12 in. diameter 1 m long cylindrical test section G. The outlet of the test pipe was sharp-edged and ended approximately .3 m inside the test section G. The return mechanism consisted of a 76 mm diameter plexiglas pipe which branched into sections I and J as shown in Figure 3. The branches I and J rejoined before returning to tank B. Flow meters were placed downstream from the two flow meters and was used in conjunction with two gate valves to calibrate the flow-meters.

The temperature of the water was monitored by two thermometers, one located at the large diameter entrance pipe D and the other at test section G. The cooling unit was not sufficient to keep the water at a constant temperature, but did limit the temperature rise to approximately 1° C/hr.

When the system was first filled, trapped air had to be released by two relief pipes located at the filter tank D and the mixing tank B.

The water had to be circulated through the system for approximately one hour before all entrained air could be released.

3.2. Hot-Film Anemometer

A hot-film anemometer and probe was the basic velocity measuring device used during the investigation. The operation, development and design of the anemometer and hot-film probe is described in detail by Ling (19). The probe is shown in Figure 4. The probe and its holder is illustrated in Figure 5. The relatively large size of the hot-film probe compared to the small dimensions of the viscous sublayer presented difficulties which will be discussed in the next chapter. An efficiently operating hot-film probe with dimensions comparable to standard hot-wire probes is not presently available.

3.3. Flow Meters

The volume rate of flow was measured by two Ramapo Flow-meters, one with a 76 mm diameter and the other with a 25 mm diameter. These meters work on the principle of drag force on a (specially contoured) body of revolution suspended in the flow stream. This force is transmitted by a rod lever and a torque tube to a four active arm strain gage bridge. The drag force measured by the unit in electrical terms was approximately proportional to the flow rate squared. The flow-meters are positioned in the system as shown in Figure 3.

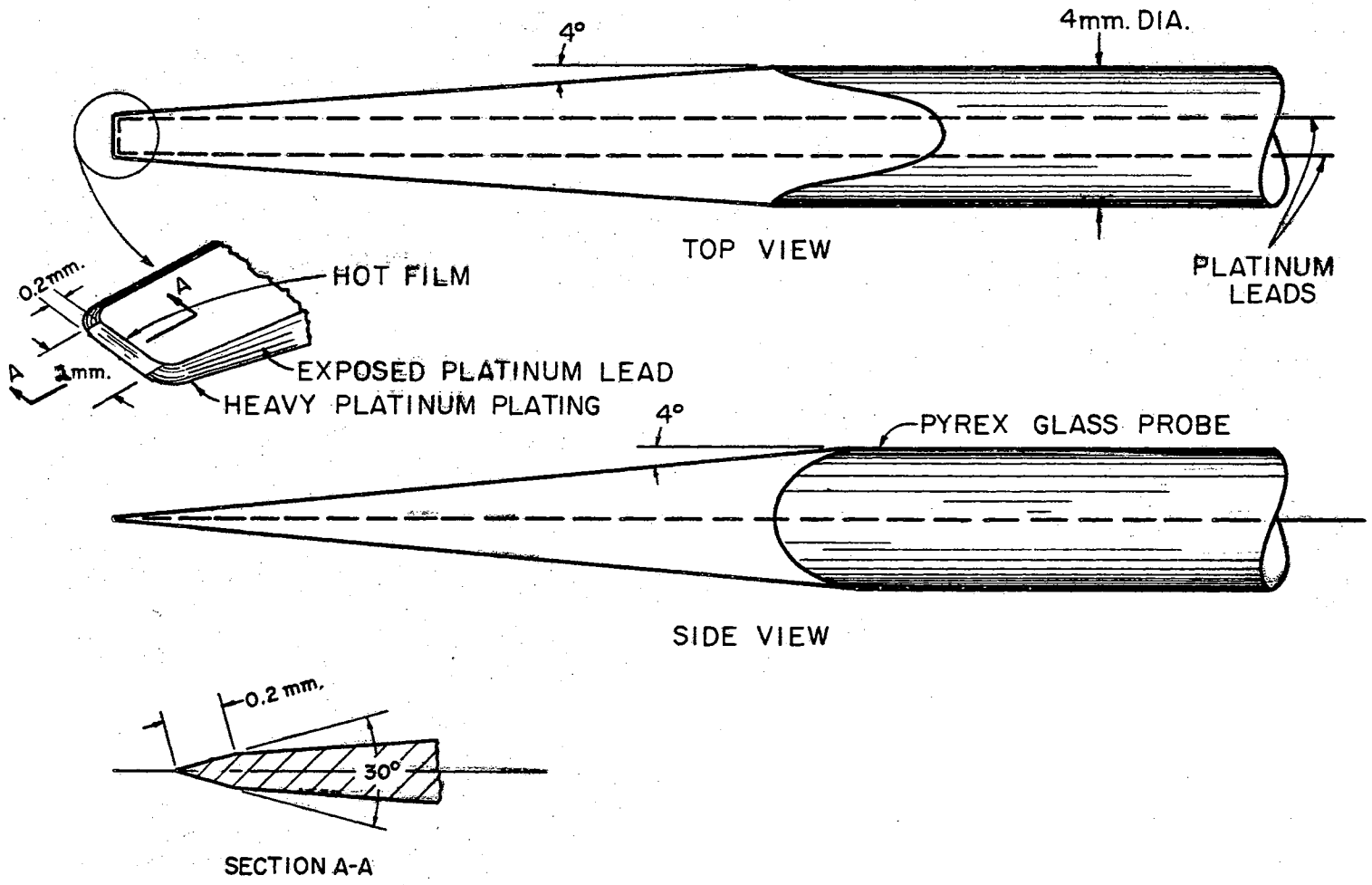

Hot Film Probe

Figure 4

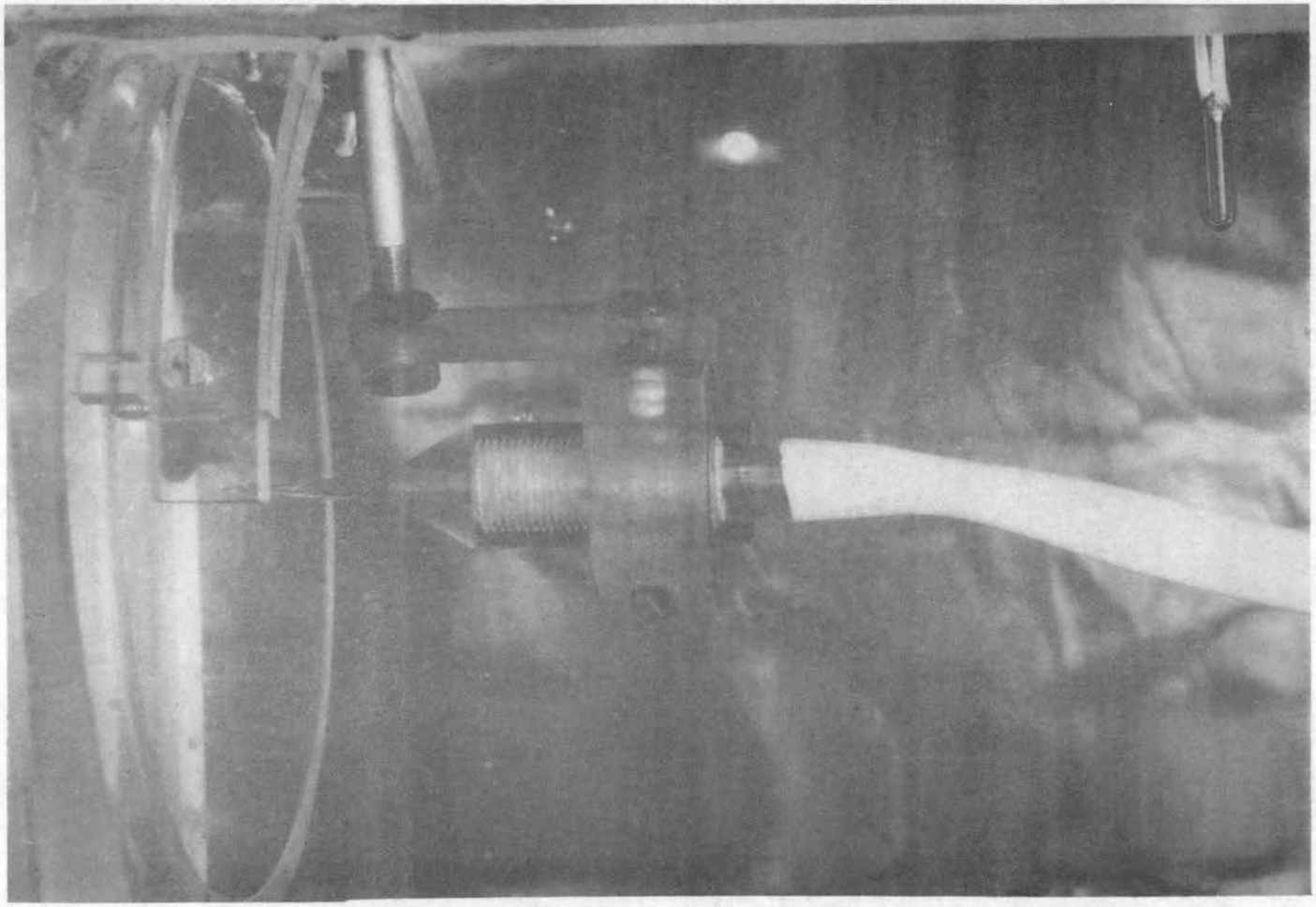

Hot Film Probe Positioned Outside Test Pipe
Outlet Cross-section with Canopy
Figure 5

3.4. Recorder

A multipoint potentiometric recorder which prints a number of variables sequentially by scanning each one individually was used as the recording device. Each variable is identified at its position by a number and a dot. There were a total of six individual printing points. Three printing points were used for the recording of the volume flow rate, and three points were used for the point velocity measurement.

The voltage from the flow-meter system was fed directly into the recorder but the voltage from the hot-film anemometer was first fed into a high impedence vacuum tube voltmeter. The voltmeter had a very high input impedance compared to the recorder and negligible drift. A voltage divider had to be used on the output amplifier to match the voltage range of the recorder. The voltmeter also permitted adjustment of the sensitivity and was especially useful in measuring small voltage differences. Figure 6 shows a block diagram of the measuring and recording devices.

3.5. Traverse Device

The positioning of the hot-film probe was accomplished by a hand operated traverse mechanism. The probe was moved along a vertical diameter at a predetermined longitudinal distance from the outlet of the test pipe as shown in Figure 7. The vertical reference distance from the hot-film probe tip to the inside test pipe wall was first set by using a 30 power stereoscopic microscope. A thin piece of paper provided a comparison for the absolute reference distance from the probe tip to the wall. The probe tip's distance, from the

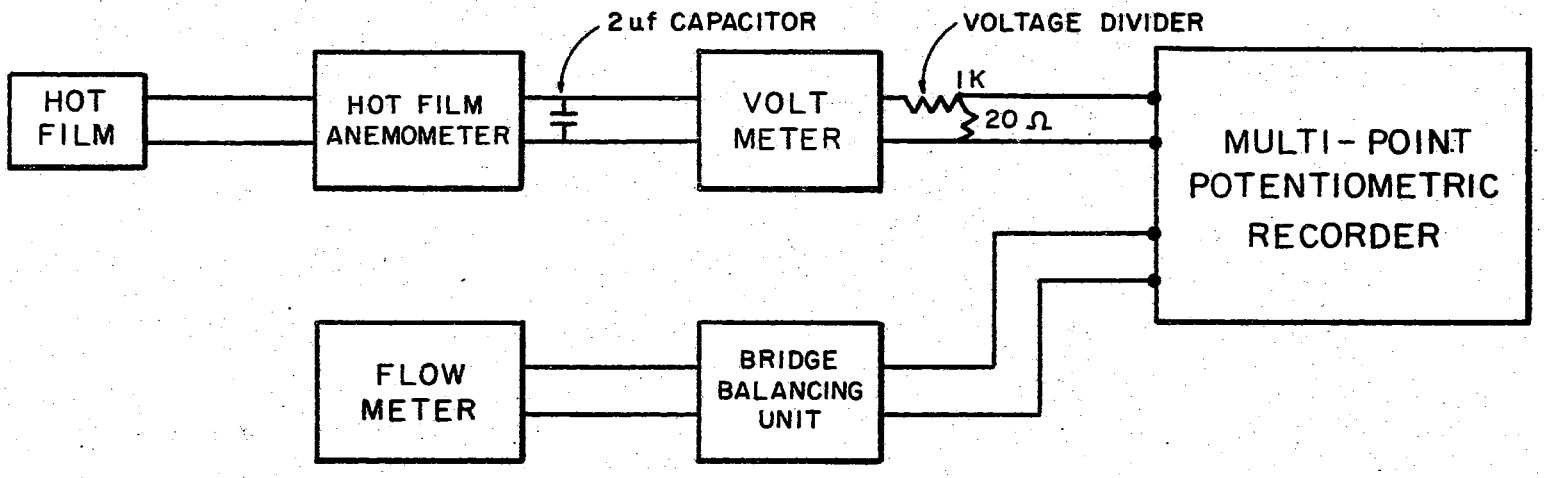
2 uf CAPACITOR
VOLTAGE DIVIDER
HOT FILM
HOT FILM ANEMOMETER
VOLT METER
1K
20 Ω
MULTI - POINT POTENTIOMETRIC RECORDER
FLOW METER
BRIDGE BALANCING UNIT

Figure 6

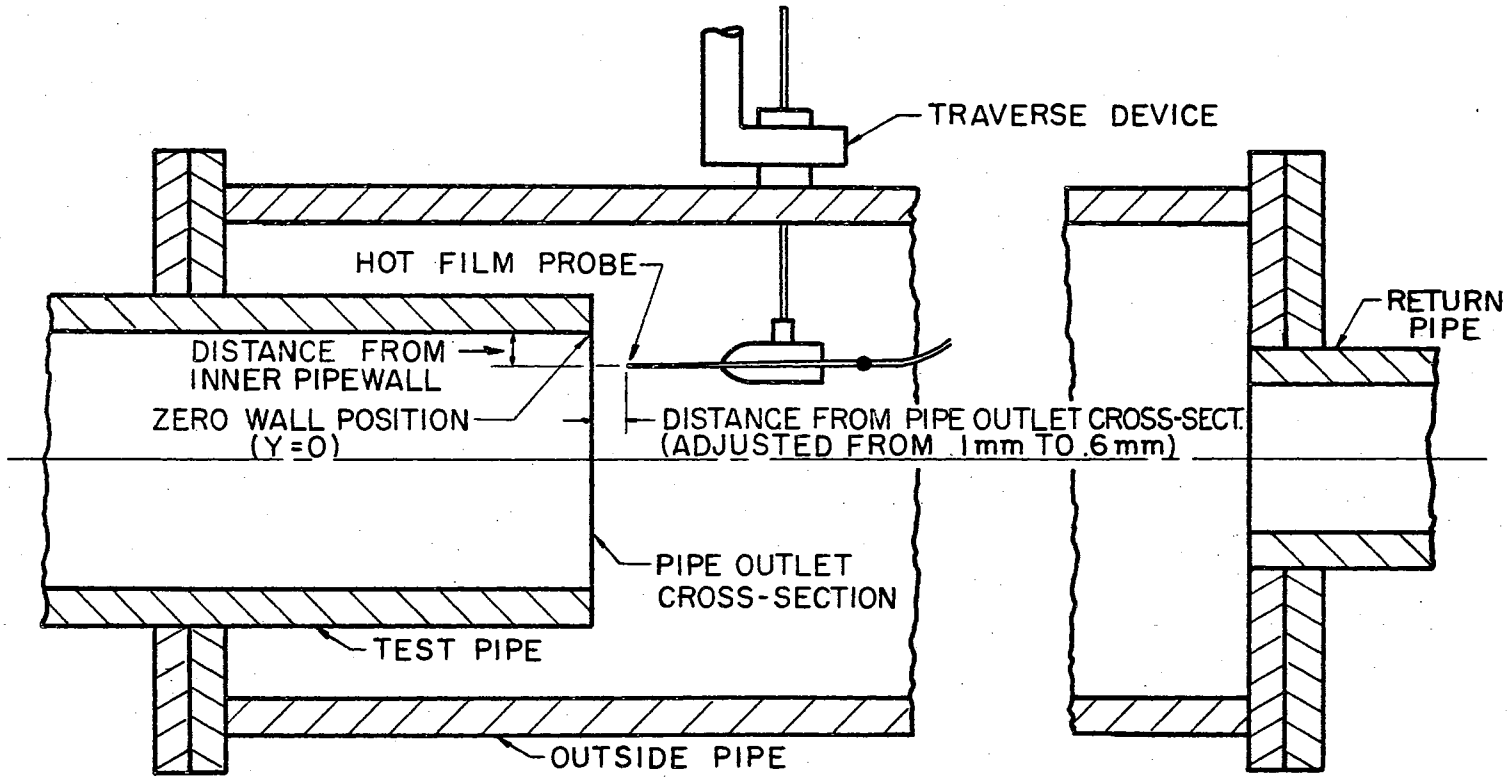
TRAVERSE DEVICE
HOT FILM PROBE
RETURN PIPE
DISTANCE FROM INNER PIPEWALL
ZERO WALL POSITION (Y=0)
DISTANCE FROM PIPE OUTLET CROSS-SECT. (ADJUSTED FROM .1mm TO .6mm)
PIPE OUTLET CROSS-SECTION
TEST PIPE
OUTSIDE PIPE

Figure 7

inner pipe wall, first set approximately at .1 mm, compared to the thin paper sheet 0.1 mm thick, gave an estimated reference accuracy of $\pm$ 0.05 mm.

For vertical distances of more than 7.6 mm from the inner wall, a vernier and scale on the traverse device was used. The scale and vernier allowed probe tip distance settings at $\pm$ 0.254 mm. For probe tip distance settings closer to the wall than 7.6 mm, a micrometer which was securely mounted on the top of the traverse device was used. This micrometer had an accuracy of $\pm$ 0.01 mm.

The horizontal distance of the probe tip to the vertical plane of the test pipe outlet was determined by a traveling telescope and a cross-hair which gave an accuracy of distance measurement of $\pm$ .03 mm.

CHAPTER IV

CALIBRATION AND EXPERIMENTAL PROCEDURES

4.1. Flow Meters

The calibration of the flow meters consisted of a measurement of the weight of water collected during a measured time interval related to the electrical output of the meter system. The water was diverted from the return mechanism by the p.v.c. two-way ball valve into a large stainless steel tank which was placed on a balance arm platform scale. The scale had an initial weight setting so that when the scale was balanced by the collected water a steady condition of flow rate from the system had been obtained. The time interval necessary to collect a specified weight of water was measured by a stop watch. The temperature of the collected water was measured and the volumetric rate of flow was calculated and plotted against the recorded electrical output of the flow metering system. Figure 8 shows a typical calibration curve.

Both the three inch flow meter and the one inch flow meter were calibrated as either the return pipes I or J could be shut off independently by the gate valves directly behind the flow meters. (See Figure 3.) The accuracy of the calibration technqiue was estimated to be within $\pm 1.5\%$

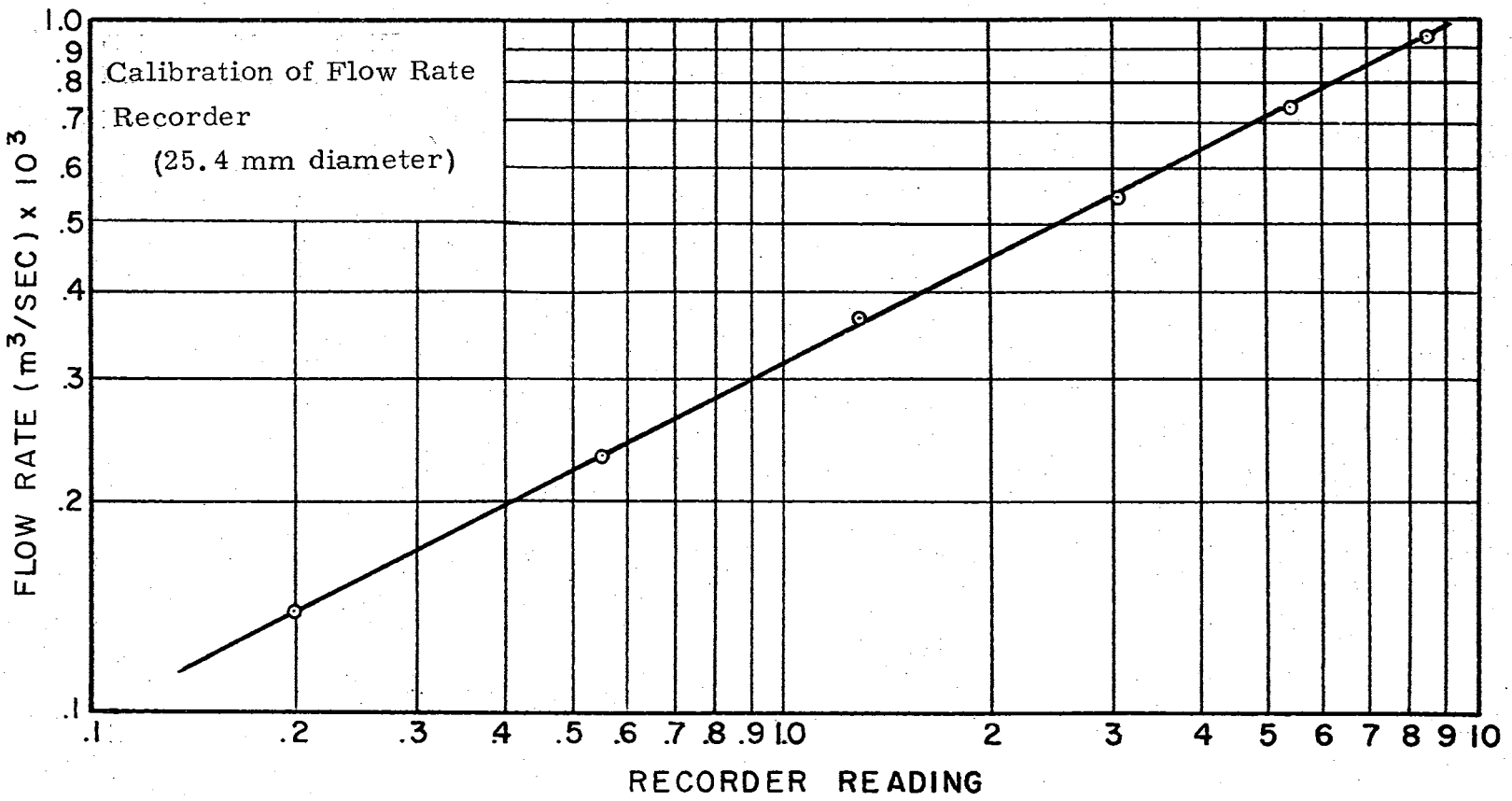
Calibration of Flow Rate
Recorder
(25.4 mm diameter)
FLOW RATE (m^3/SEC) x 10^3
1.0
.9
.8
.7
.6
.5
.4
.3
.2
.1
.1
.2
.3
.4
.5
.6
.7
.8
.9
1.0
2
3
4
5
6
7
8
9
10
RECORDER READING

Figure 8

4.2. Calibration of the Hot-Film Anemometer and Probe for Low Velocities

For flow velocities less than 100 mm/sec., a tow tank device was used to calibrate the hot-film system. Figure 9 shows the tow tank, the hot-film probe, and the holder. The probe was moved through the water by a force transmitted along a string. The string was attached to a piston which descended in a vertical 1 m long brass cylindrical pipe filled with water. The pistons had a concentric hole bored throughout their length so that various sized orifice plates could be fitted over the hole permitting variation in the velocity at which the probe was towed. The probe was timed through a 30 cm distance located near the center of the tow tank length. Except for minor deviations due to friction in the towing device, a constant velocity of the probe over this length was observed. Because of friction, however, the lowest probe velocity measured with consistent results was 2 mm/sec. The length of the tank limited the maximum velocity observed to 100 mm/sec. The output of the anemometer during the calibration test was converted directly to recorder reading. Figure 10 shows the relationship between the probe velocity and the recorder reading. Also in Figure 11 the corresponsing relationship between actual voltage of the anemometer and the recorder reading is shown.

As mentioned in Section 3.1, the temperature of the distilled water used in the water tunnel steadily increased during the tests. Since the hot-film anemometer was temperature sensitive, the calibration tests were run at various temperatures so that the water temperature during the actual tests would be within the temperature

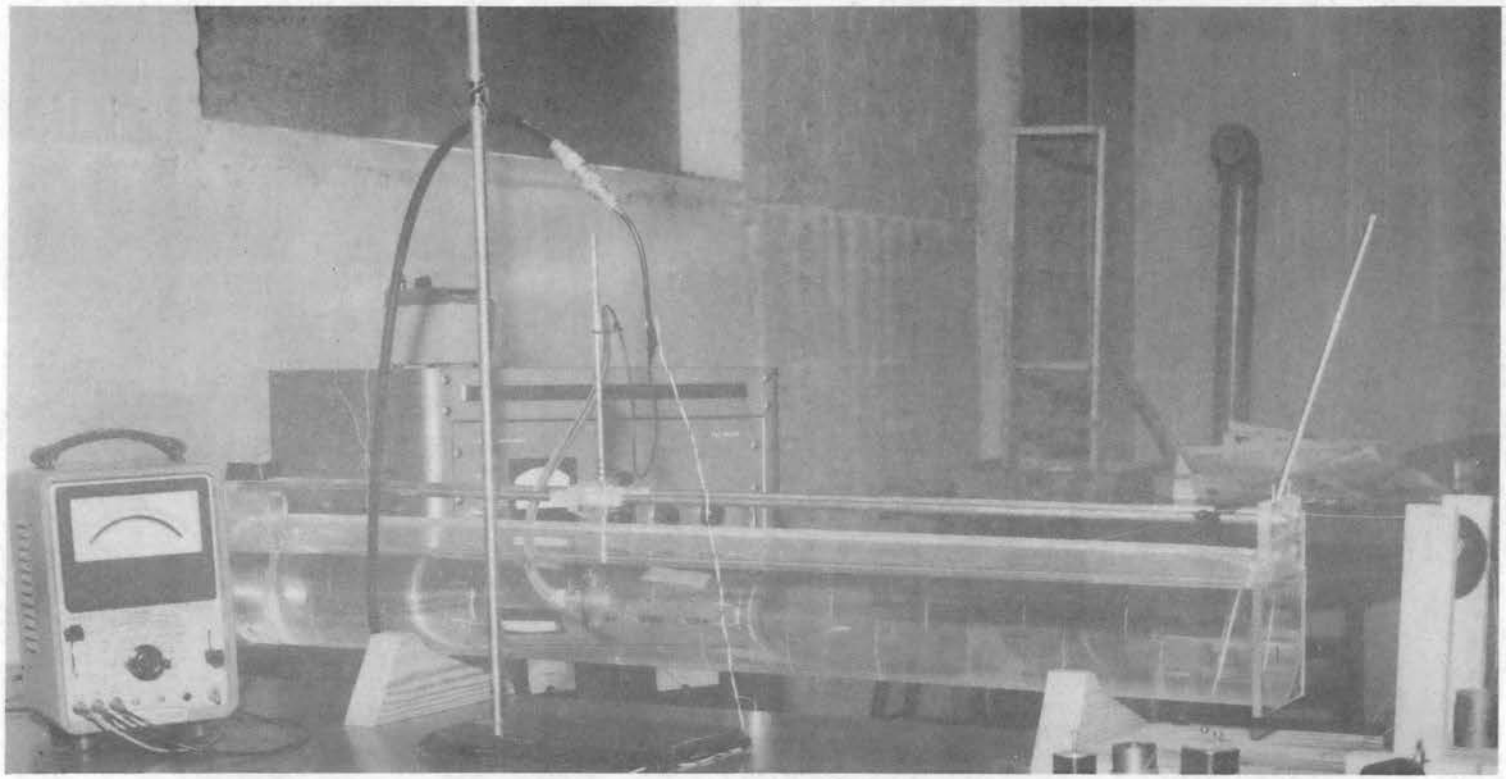

Tow Tank Device
Figure 9

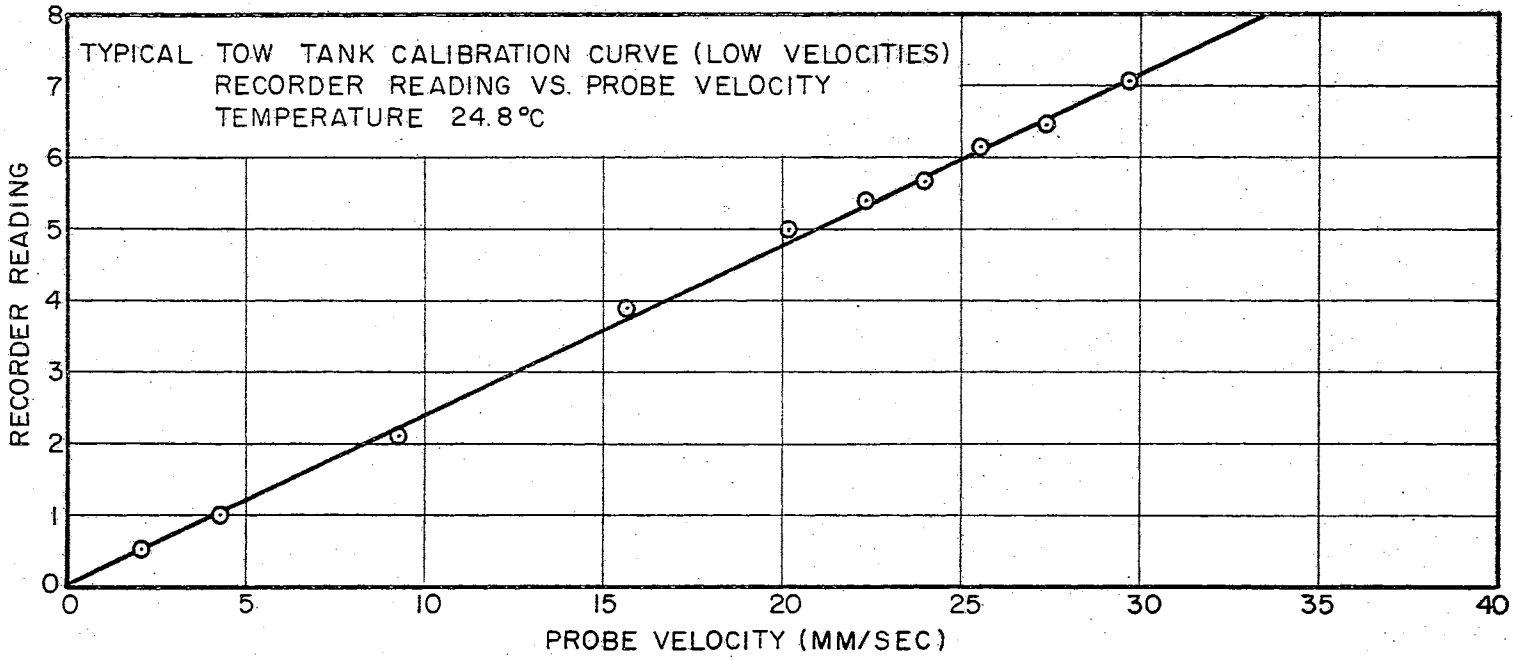
TYPICAL TOW TANK CALIBRATION CURVE (LOW VELOCITIES)
RECORDER READING VS. PROBE VELOCITY
TEMPERATURE 24.8°C
RECORDER READING
PROBE VELOCITY (MM/SEC)
0
1
2
3
4
5
6
7
8
0
5
10
15
20
25
30
35
40

Figure 10

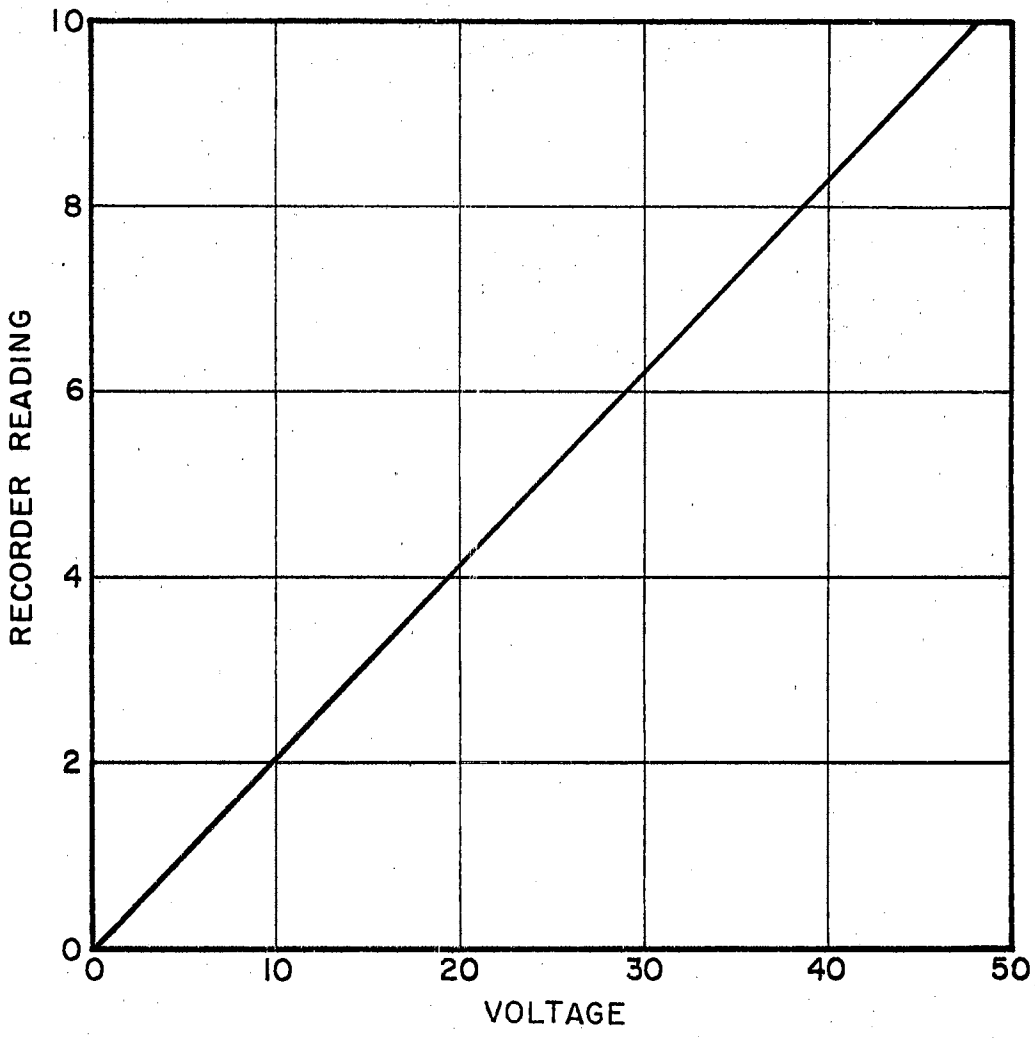

Figure 11

range of the calibration results. Figure 12 shows the calibration curve for various temperatures when the tow tank was used.

4.3. Calibration of the Hot-Film Anemometer and Probe for High Velocities

For calibration of the probe for velocities over 100 mm/sec. to 450 mm/sec., the probe was placed in the test section of the water tunnel. The probe was positioned such that it was parallel to the longitudinal axis of the pipe and the hot-film tip of the probe was exactly in the center of the test pipe outlet. The probe in this position theoretically measured the maximum mean velocity of flow.

From the power law, $\frac{u}{U_m} = (\frac{y}{R})^{\frac{1}{n}}$ (where the exponent n is dependent on the Reynolds Number). Define $\overline{U}$ as volume rate of flow per cross-sectional area. Then

$$A\overline{U} = Q = \int_0^R 2\pi U_m (\frac{y}{R})^{\frac{1}{n}} (R - y)dy$$

Integrating the equation for Q,

$$\pi R^2 \overline{U} = \frac{U_m R^{\frac{1}{n}+1} 2\pi}{(\frac{1}{n}+1) R^{\frac{1}{n}-1}} - \frac{U_m R^{\frac{1}{n}+2} 2\pi}{(\frac{1}{n}+2) R^{\frac{1}{n}}}$$

and

$$\frac{1}{(\frac{1}{n}+1)} - \frac{1}{(\frac{1}{n}-1)} = \frac{\overline{U}}{2U_m}$$

then

$$\frac{\overline{U}}{U_m} = \frac{2n^2}{(1+n)(1+2n)} . \qquad (4\text{-}3.1)$$

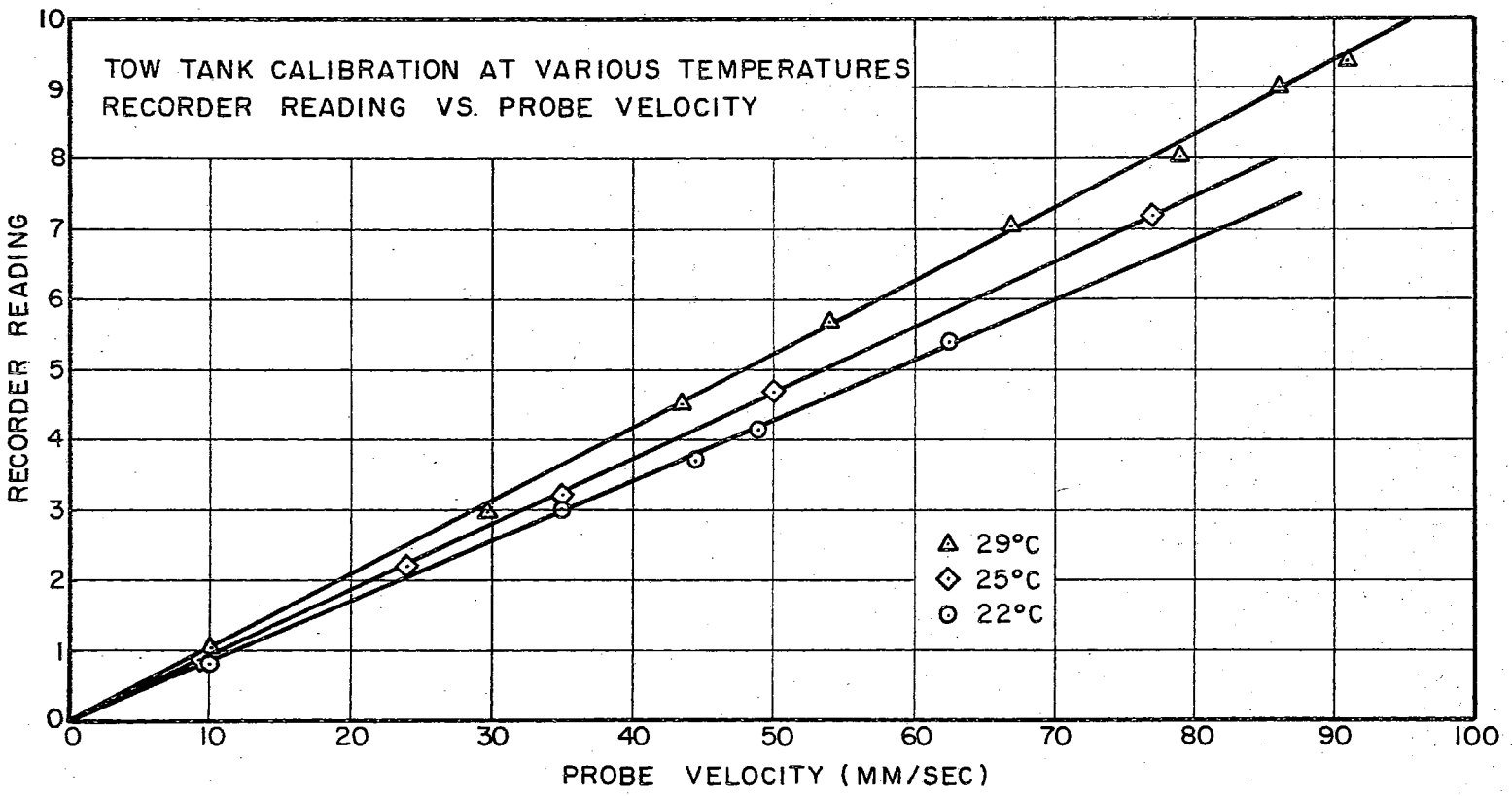
TOW TANK CALIBRATION AT VARIOUS TEMPERATURES
RECORDER READING VS. PROBE VELOCITY
RECORDER READING
PROBE VELOCITY (MM/SEC)
29°C
25°C
22°C
0
1
2
3
4
5
6
7
8
9
10
0
10
20
30
40
50
60
70
80
90
100

Figure 12

Since n depends on Reynolds Number, it must be determined from experimental data. Schlichting supplies such data on p. 505 (20), where $n = 6.6$ for $R = 23,000$ and $n = 7.0$ for $R = 110,000$. Therefore, when

$$n = 6.6 \qquad \frac{\overline{U}}{U_m} = .808$$

$$n = 7.0 \qquad \frac{\overline{U}}{U_m} = .817 \ .$$

For calibration purposes, a constant value of $\frac{\overline{U}}{U_m} = .800$ was used to relate the volume rate of flow Q as measured from the flow meters to U_m, that is,

$$\overline{U} = \frac{Q}{A} = .8\, U_{max} . \qquad (4\text{-}3.2)$$

This introduced a maximum error of 2% in calibration (but it was only necessary to use this for determining velocities of 100 mm/sec. or over). Figure 13 shows a typical calibration curve obtained for high velocity flow.

4.4. Experimental Procedure

Before the actual mean velocity tests were run, a check on the symmetry of the velocity profile was carried out. In the region of laminar flows the profile was not symmetrical, although the turbulent velocity profile did indicate a symmetrical distribution. Transition from laminar flow accured about Re = 2200 with continuous turbulence being observed for Re greater than 3000. All previous

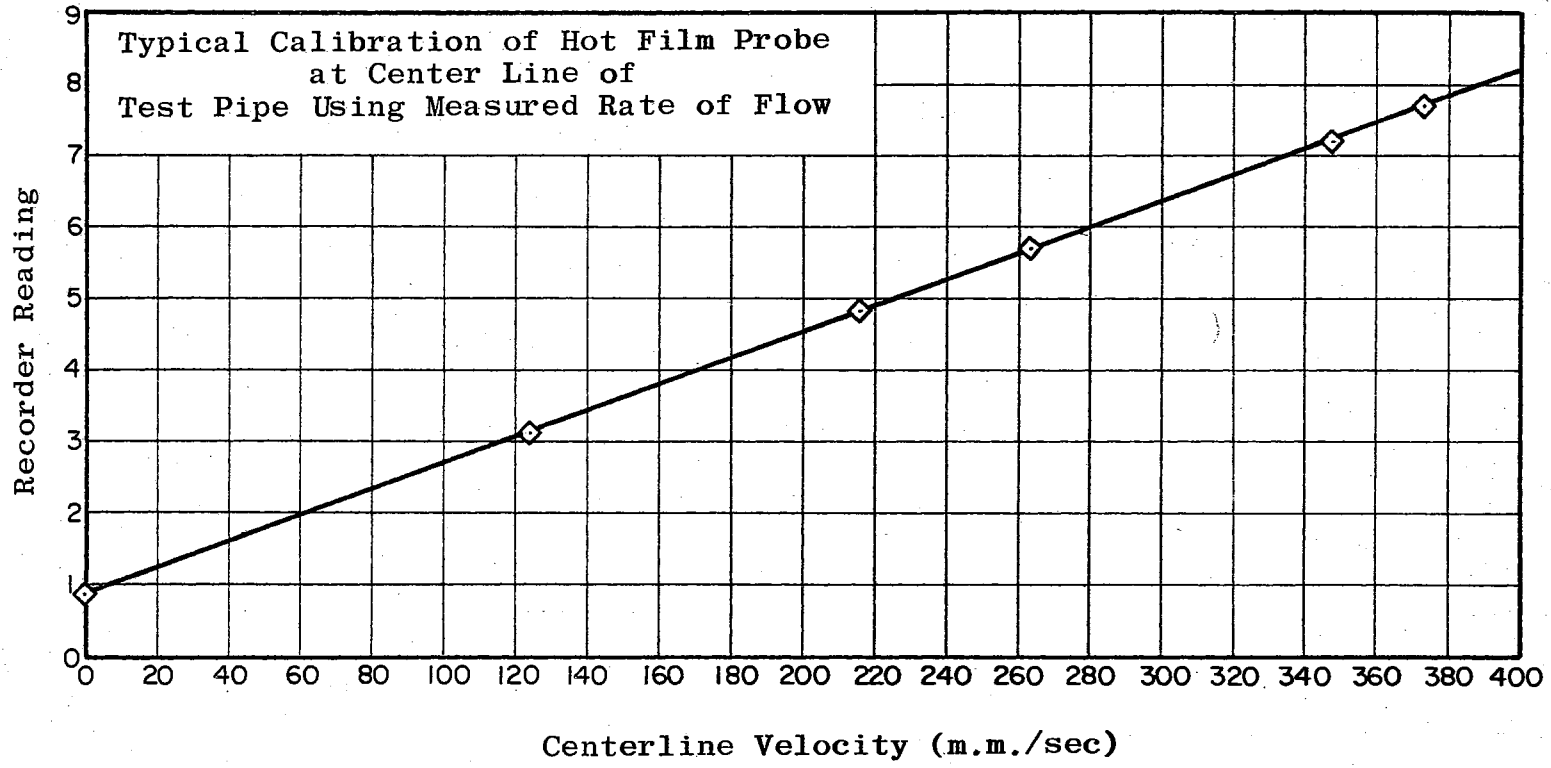
Typical Calibration of Hot Film Probe
at Center Line of
Test Pipe Using Measured Rate of Flow
Recorder Reading
0
1
2
3
4
5
6
7
8
9
0 20 40 60 80 100 120 140 160 180 200 220 240 260 280 300 320 340 360 380 400
Centerline Velocity (m.m./sec)

Figure 13

experimental evidence indicates that for Reynold Numbers 5000 and over, a fully developed turbulent velocity profile exists after an inlet length of under 100 diameters. It was assumed that fully developed turbulent flow existed at the outlet of the test pipe which was 186 diameters from the inlet in the present study.

The hot-film probe was positioned at the center of the pipe outlet as indicated in Section 4.3 at the start of each test. By comparing the velocity determined by the flow rate measuring devices with the velocity found with the calibration curve (see Section 4.3) a check was made on the relative accuracy of the measurement. An even better check was determined if the velocity measured was less than 100 mm/sec, that is, the velocity found from using the flow rate reading could be compared to the velocity determined from the tow tank calibrations.

The voltage output of the hot-film system was recorded for a time interval for each position of the probe. The duration of the recording at a certain position was a function of the time necessary to develop stationary output. This time varied between one and five minutes except when drift occured. The probe tip was located in cross-sectional planes parallel to the test pipe outlet cross-section. The probe tip was moved along a vertical diameter in these planes from a position in the center of the pipe to positions behind the test pipe wall. Figure 7 illustrates the positioning of the probe and probe tip.

CHAPTER V

RESULTS AND CONCLUSIONS

The experimental work was carried out in three main series of tests. In each series dimensionless velocity profiles were obtained for tests corresponding to Reynolds numbers of approximately 5,000, 10,000, 28,000 and 50,000.

The first series of tests were conducted with the probe tip located outside the pipe outlet cross-section. The distance of the tip to the pipe outlet cross-section varied from 0.1 mm to 0.6 mm.

In the second series of tests, the probe tip was inserted 3 mm into the test pipe, that is, the probe was located in a cross-section 3 mm inside the pipe outlet cross-section.

A type of canopy was used in the third series of tests attempting to eliminate wall interference and jet diffusion effects and yet provide the same type of conditions existing for tests with the probe inserted into the pipe.

The three series of tests will be individually discussed in detail in the following sections.

5.1. Tests with the Probe Located Outside the Pipe Outlet Cross-Section

Dimensionless velocities profiles corresponding to four Reynolds numbers are shown in Figure 14 and Figure 15. The probe tip was located at distances outside the pipe outlet of 0.1 mm for test 14

and 0.3 mm for test 15. In each figure, the straight line corresponds to Nikuradse's experimental results ($\frac{u}{u^*} = 5.75 \log_{10} + 5.5$) and the curved line represents a linear variation of velocity with distance.

As can be noted in Figure 14 the results for the three lower Reynold's numbers 5900, 10,000, and 27,000 indicate slightly lower values in the logarithmic region when compared to Nikuradse's results but the tests at Re = 26,000 and Re = 48,000 definitely deviate from the straight line relationship in the core region as predicted by the "Law of the Wake". All the test results show a marked trend toward the linear variation of velocity with distance near the wall. However, the tests also indicate a slight dependence on Reynolds number as the probe approaches the wall. Increasing the Reynold's number caused a greater deviation from the linear variation of velocity with distance, that is, a higher than predicted value of velocity for small distances from the wall. The large differences between the logarithmic relationship $\frac{u}{u^*} = 5.75 \log_{10} + 5.5$ and the test results at Re = 48,000 around $\frac{yu^*}{\nu} = 2.2$ persisted when checked. Although, the deviation does not appear in later tests at that same Reynold's number.

The results for test 15 again indicate values lower than Nikuradse's in the logarithmic region except that the large differences noted for the previous high Reynold's number test Re = 48,000 have disappeared for the test Re = 51,500. Results in the core area follow the "Law of the Wake" for both high Reynold's number tests Re = 51,500 and Re = 25,400. Near the wall, however, there were large deviations from the linear velocity profile more pronounced than in the 0.1 mm test. Dependence on Reynold's number can be noted for all

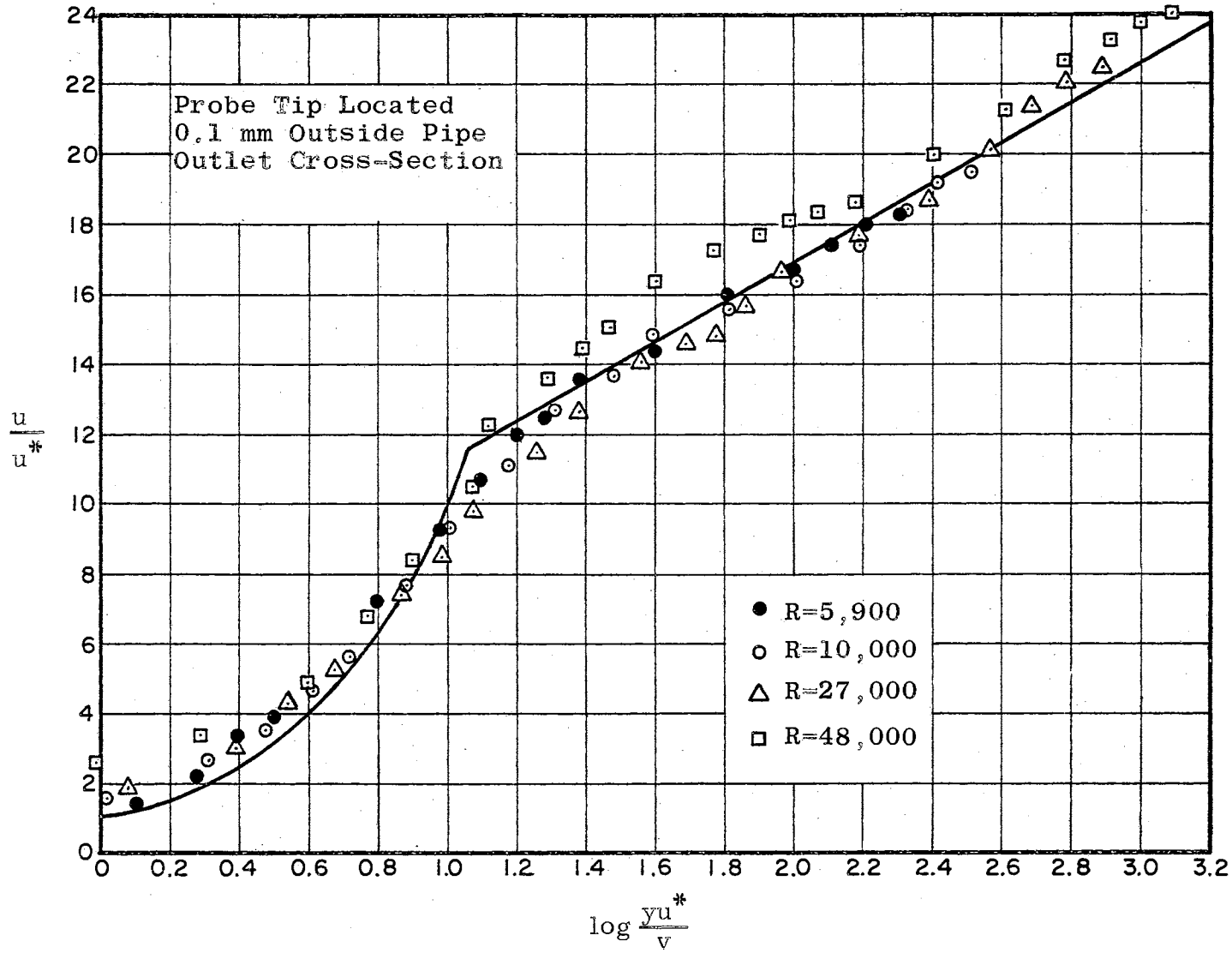
Probe Tip Located
0.1 mm Outside Pipe
Outlet Cross-Section
R=5,900
R=10,000
R=27,000
R=48,000
u/u*
log yu*/v
0
2
4
6
8
10
12
14
16
18
20
22
24
0
0.2
0.4
0.6
0.8
1.0
1.2
1.4
1.6
1.8
2.0
2.2
2.4
2.6
2.8
3.0
3.2

Figure 14

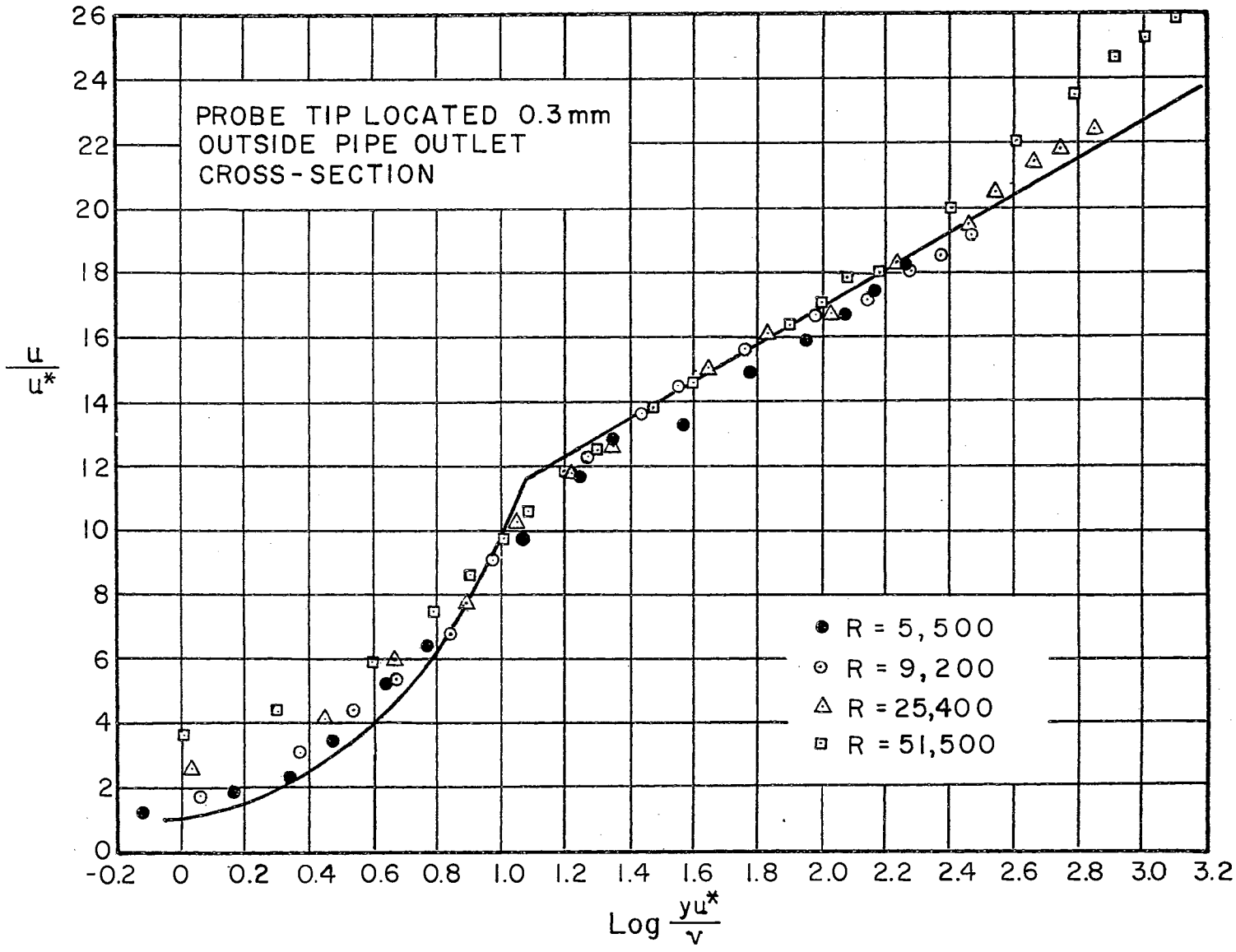
PROBE TIP LOCATED 0.3mm
OUTSIDE PIPE OUTLET
CROSS-SECTION
R = 5,500
R = 9,200
R = 25,400
R = 51,500
u/u*
Log yu*/ν
26
24
22
20
18
16
14
12
10
8
6
4
2
0
-0.2
0
0.2
0.4
0.6
0.8
1.0
1.2
1.4
1.6
1.8
2.0
2.2
2.4
2.6
2.8
3.0
3.2

Figure 15

but the core area. Since the "Law of the Wall" excludes dependence directly on Reynold's number, these tests seem to contradict this basic hypothesis.

Noting a change in velocity results with a change in the probe tip's horizontal distance from the outlet cross-section, another series of tests were run at probe tip distances of 0.2 mm, 0.4 mm and 0.6 mm. Figures 16, 17, 18, 19 and 20 give the results of these tests in terms of velocity and distance (contrasting with the usual $\frac{u}{u^*}$ vs. $\frac{u^*y}{\nu}$ plots). All of the test results indicate a finite velocity at the inner surface of the wall ($y = 0$, where the center of the probe tip is directly in line with the inner surface of the test pipe). Furthermore, the results indicate a finite velocity at positions of the probe tip completely shielded from direct flow. This velocity indication however, seemed to reach a constant value at $y = -.35$ to $y = -0.40$ mm (negative values indicating positions of the probe tip beyond $y = 0$). It could be assumed that the velocity measured at the positions of the probe tip $y = 0$ was too high by an amount equal to the "background velocity" (the constant velocity measured by the probe beyond $y = -0.35$ mm). It was also assumed that the influence of the "background velocity" extended away from wall inner surface the same distance that it took to reach equilibrium behind the wall. The velocity for positions $y = 0$ to approximately $y = 0.35$ was assumed too large by an amount proportional to the distance from $y = 0$, that is,

$$u_{corr} = \frac{0.35 - y}{0.35} u_{background} \cdot \qquad 5\text{-}1.1$$

A dashed line in the Figures 16 to 20 represent the correct velocity values. Only the two high Reynold's number tests were corrected in the figures, as the "background velocity" for the two lower Reynold's number tests was negligibly small.

Even with these corrections, the tests still indicate a finite velocity at the wall position $y = 0$. Figure 21 shows this "wall velocity" and its relationship to horizontal distance of the probe tip from the outlet cross-section. There is a definite decrease in the wall velocity from the test at 0.2 mm to the test at 0.1 mm, thus making the extension of results of a finite "wall velocity" to the actual wall position ($y = 0$, horizontal distance equal to zero) hard to define.

5.2. Results from Tests with the Probe Tip 3 mm Inside the Pipe Outlet Section

The present theories on the mean velocity distribution in straight pipe (see Chapter II) concern velocities inside the pipe rather than at the outlet cross-section. Therefore a series of tests were run with the probe tip positioned inside the pipe. These tests provided a comparison between velocities measured inside the pipe with velocities measured at various distances from the outlet cross-section.

However, the results from tests with the probe tip extending 3 mm inside the pipe outlet section exhibited the greatest wall effect on the heat transfer characteristics on the probe hot film. A preliminary correction for heat transfer effects of the wall on the hot-film in still water was determined. Figure 22 shows the results of this check. Because of the size of the probe tip, it was not possible to position the tip closer than 0.35 mm from the inner wall surface. Figure 23 gives

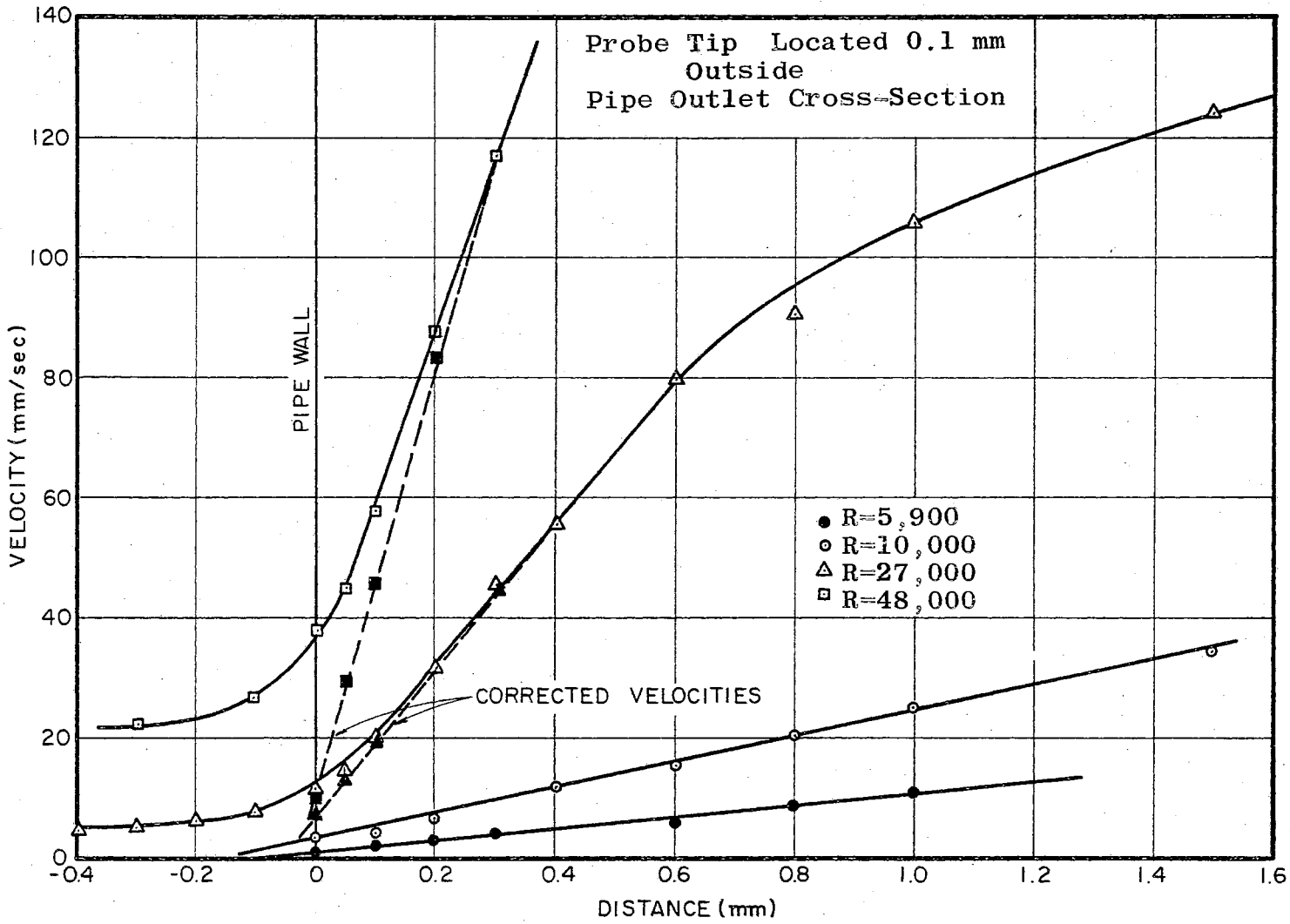
Probe Tip Located 0.1 mm
Outside
Pipe Outlet Cross-Section
PIPE WALL
CORRECTED VELOCITIES
● R=5,900
⊙ R=10,000
△ R=27,000
□ R=48,000
VELOCITY (mm/sec)
DISTANCE (mm)
140
120
100
80
60
40
20
0
-0.4
-0.2
0
0.2
0.4
0.6
0.8
1.0
1.2
1.4
1.6

Figure 16

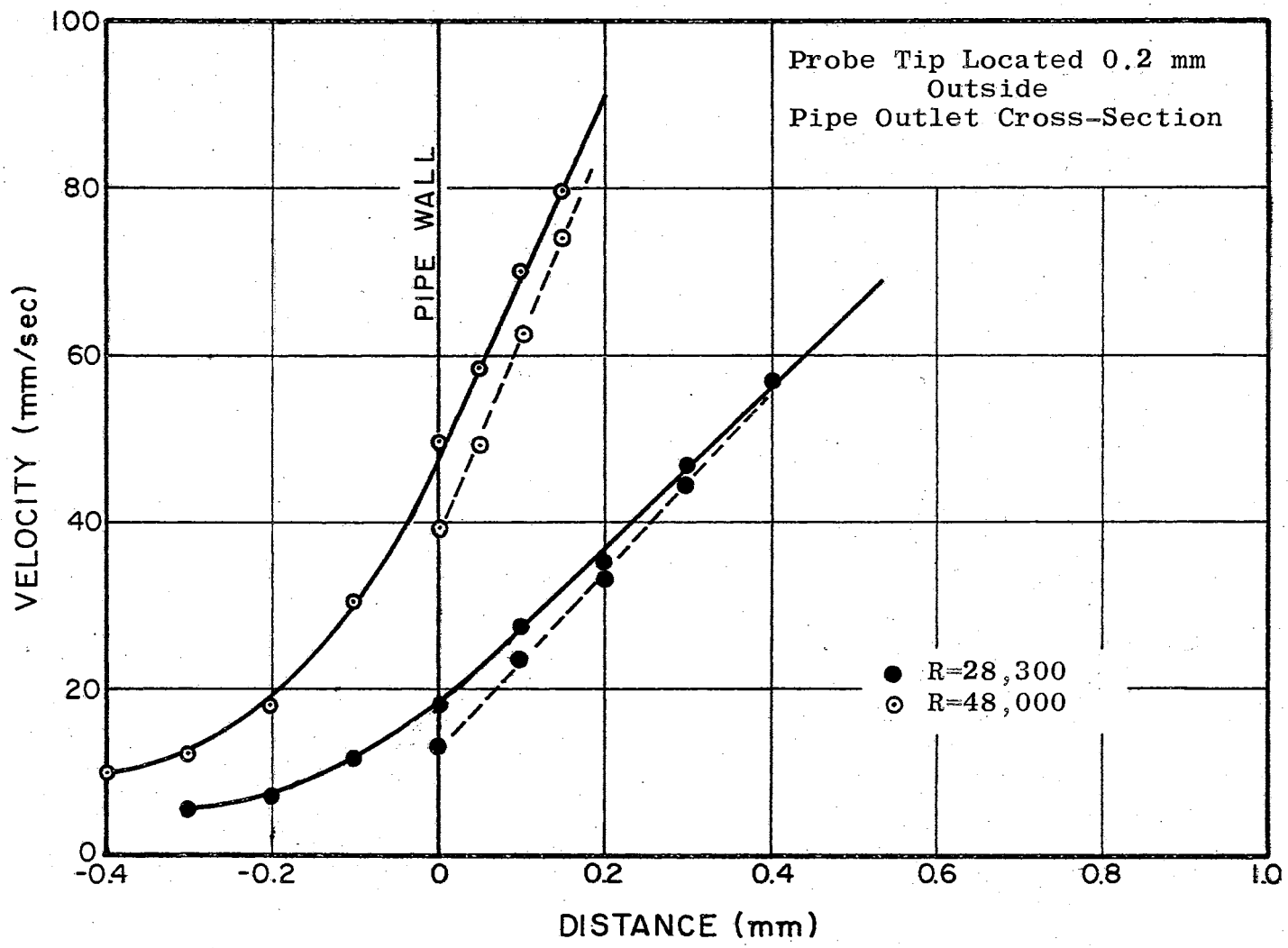
Probe Tip Located 0.2 mm
Outside
Pipe Outlet Cross-Section
PIPE WALL
R=28,300
R=48,000
VELOCITY (mm/sec)
DISTANCE (mm)
100
80
60
40
20
0
-0.4
-0.2
0
0.2
0.4
0.6
0.8
1.0

Figure 17

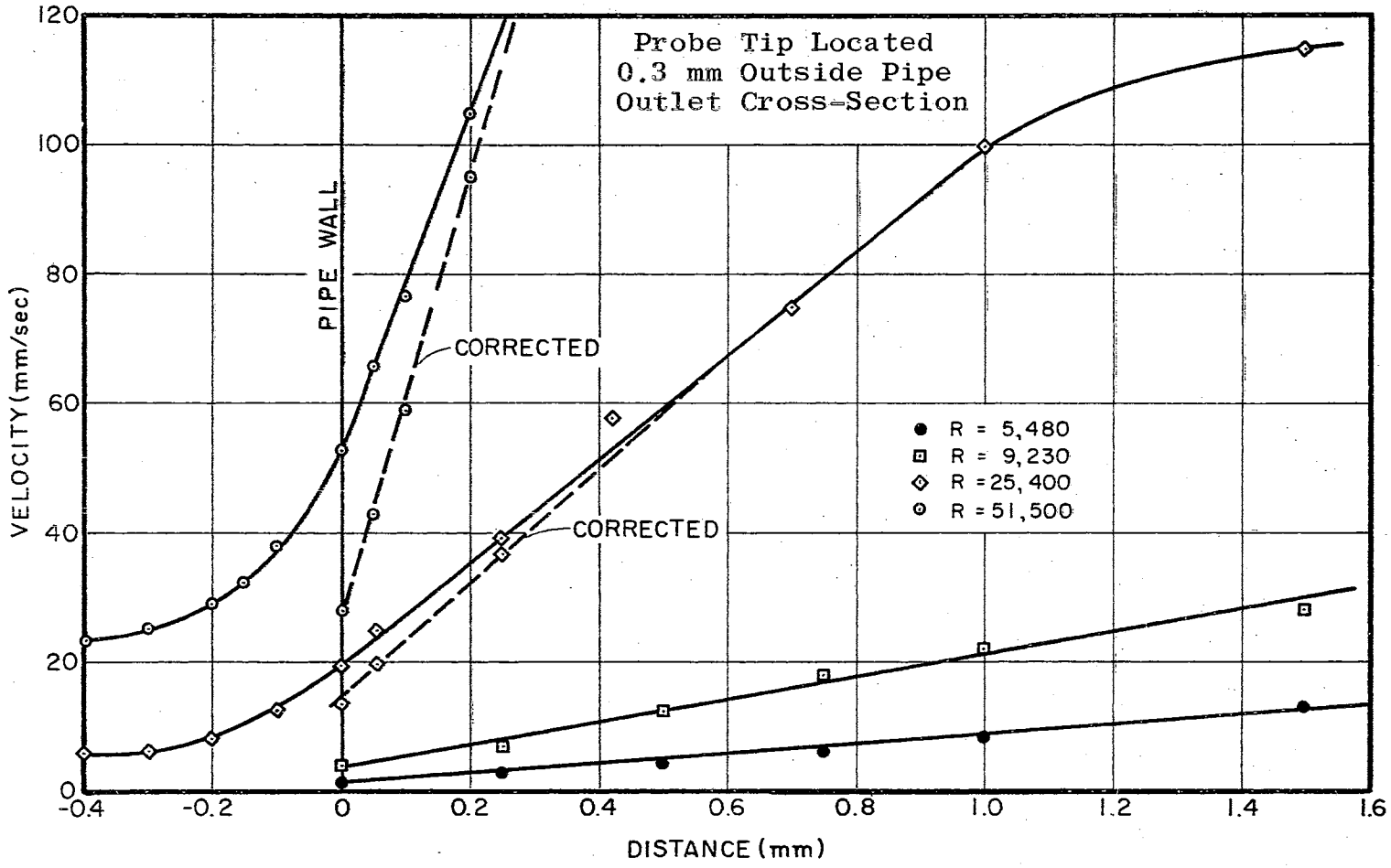
Probe Tip Located
0.3 mm Outside Pipe
Outlet Cross-Section
PIPE WALL
CORRECTED
CORRECTED
R = 5,480
R = 9,230
R = 25,400
R = 51,500
VELOCITY (mm/sec)
DISTANCE (mm)
120
100
80
60
40
20
0
-0.4
-0.2
0
0.2
0.4
0.6
0.8
1.0
1.2
1.4
1.6

Figure 18

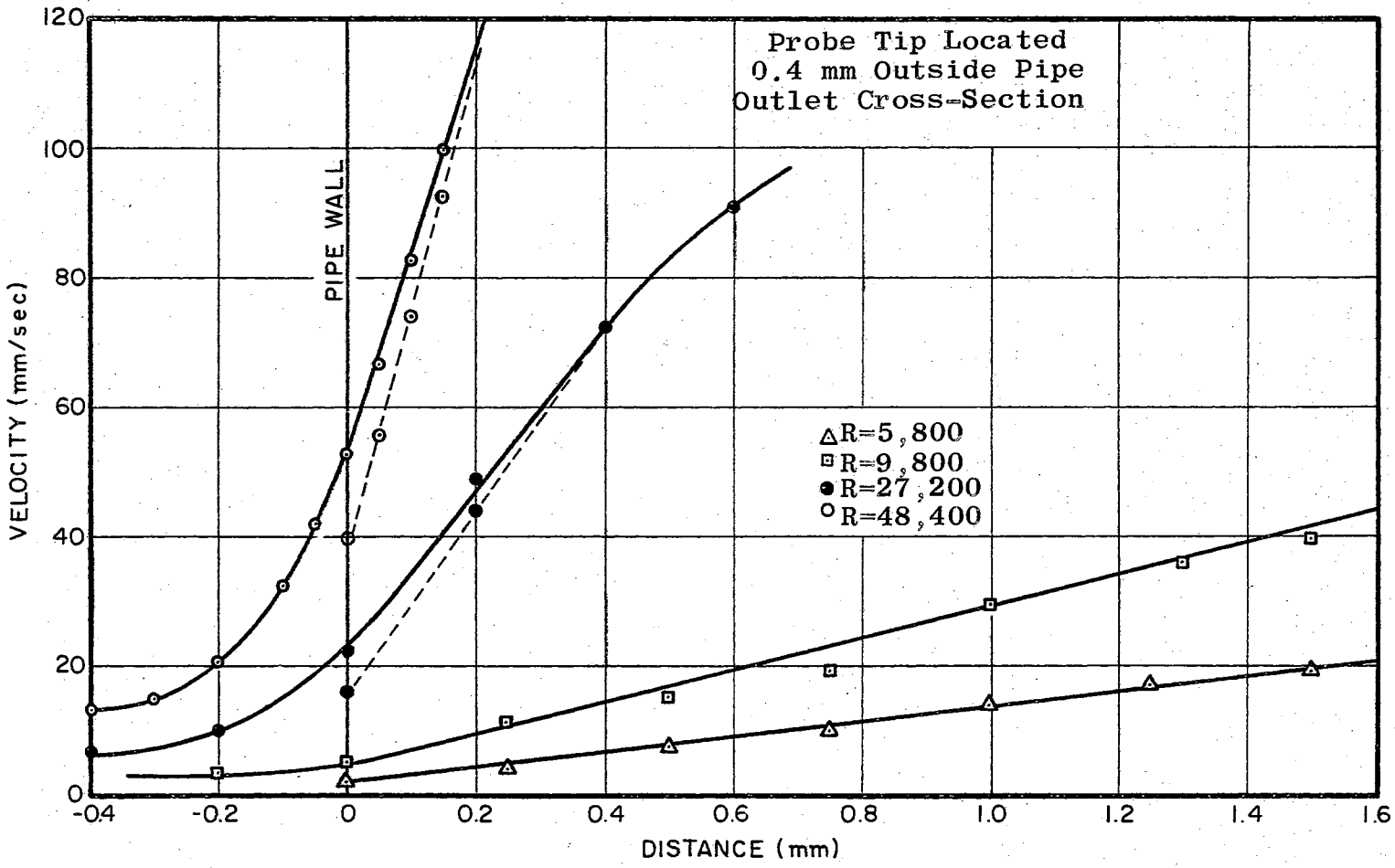
Probe Tip Located
0.4 mm Outside Pipe
Outlet Cross-Section
PIPE WALL
△R=5,800
□R=9,800
●R=27,200
○R=48,400
VELOCITY (mm/sec)
DISTANCE (mm)
0
20
40
60
80
100
120
-0.4
-0.2
0
0.2
0.4
0.6
0.8
1.0
1.2
1.4
1.6

Figure 19

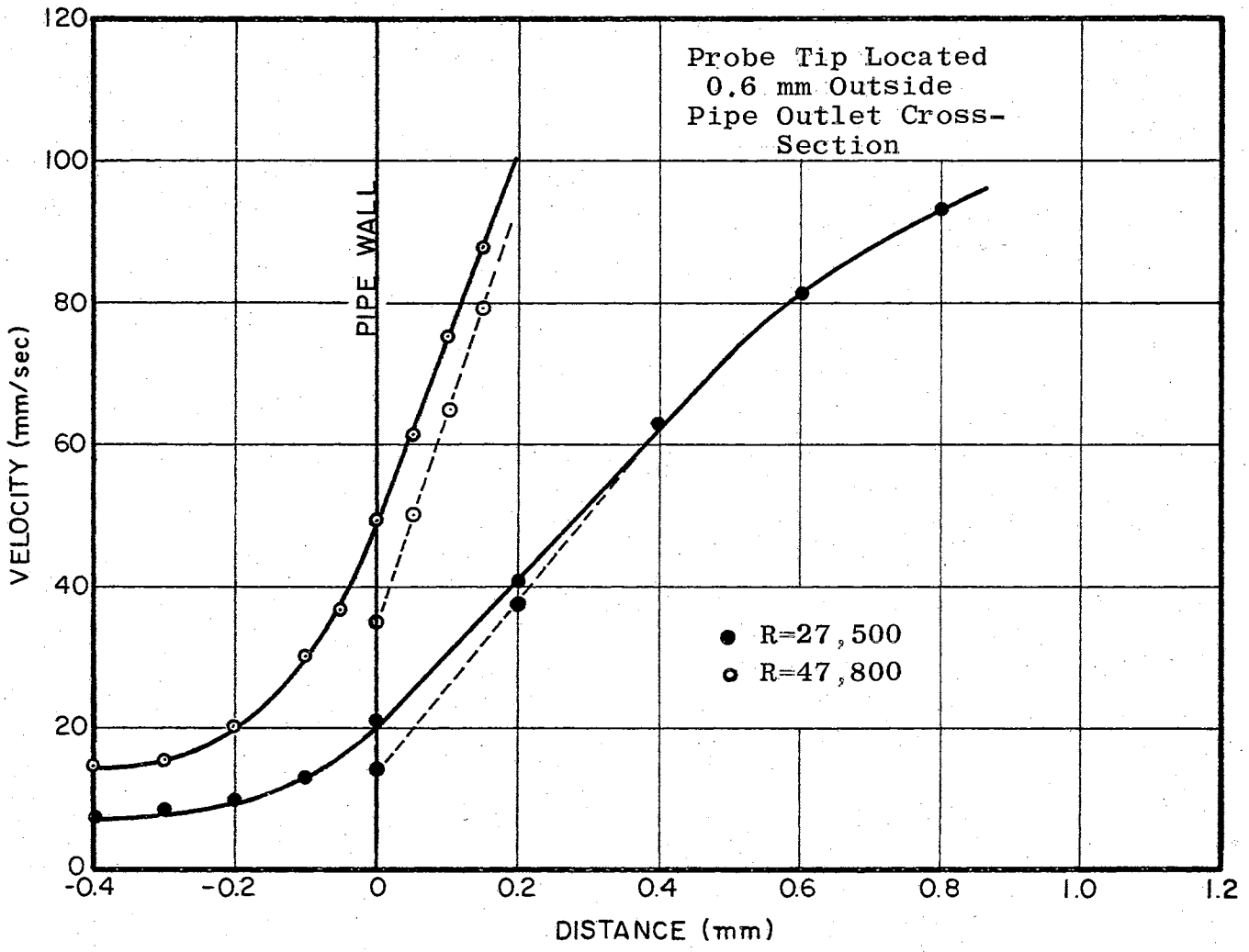
Probe Tip Located
0.6 mm Outside
Pipe Outlet Cross-
Section
PIPE WALL
R=27,500
R=47,800
VELOCITY (mm/sec)
DISTANCE (mm)
120
100
80
60
40
20
0
-0.4
-0.2
0
0.2
0.4
0.6
0.8
1.0
1.2

Figure 20

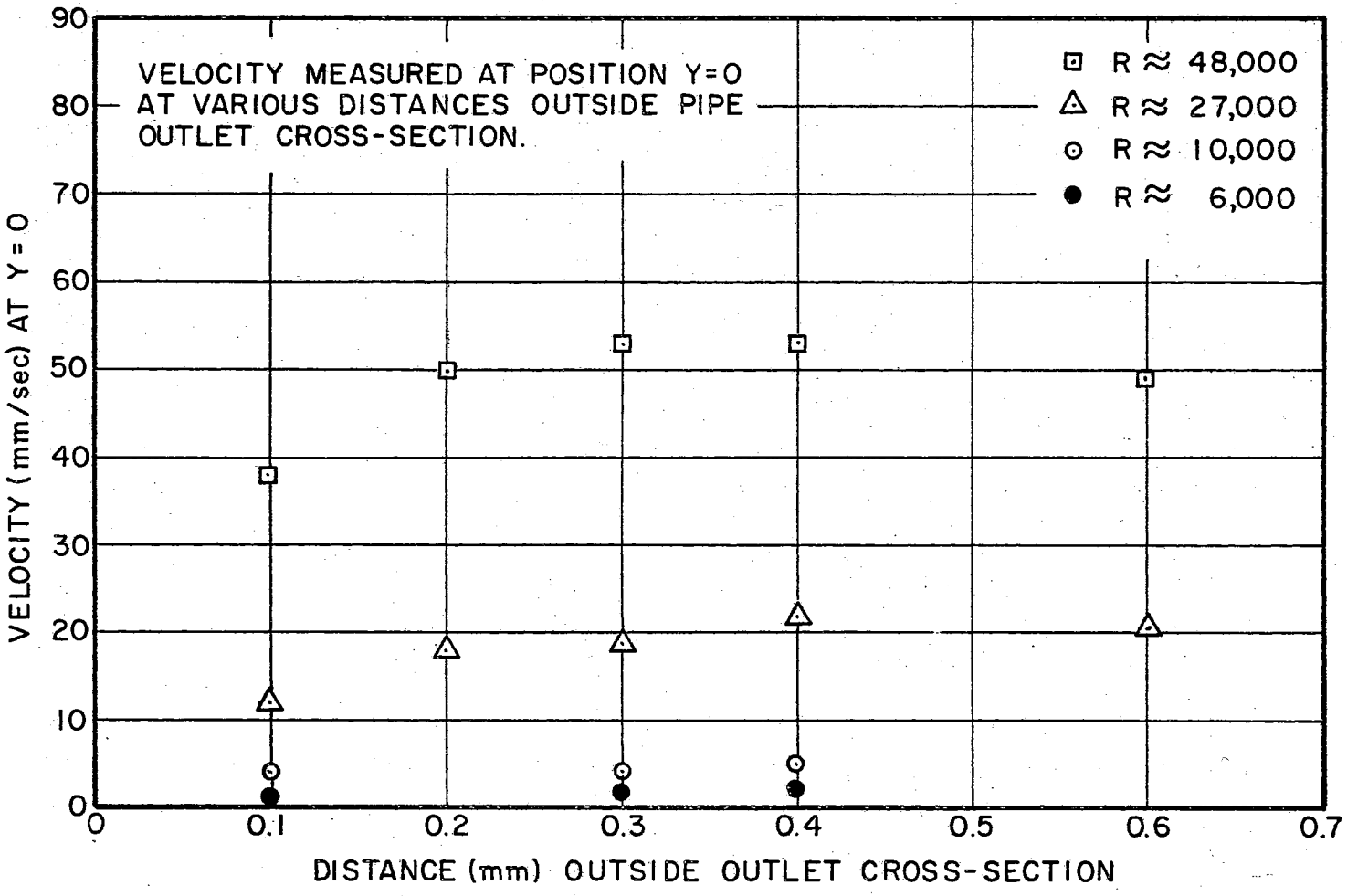
VELOCITY MEASURED AT POSITION Y=0
AT VARIOUS DISTANCES OUTSIDE PIPE
OUTLET CROSS-SECTION.
R ≈ 48,000
R ≈ 27,000
R ≈ 10,000
R ≈ 6,000
VELOCITY (mm/sec) AT Y = 0
90
80
70
60
50
40
30
20
10
0
0
0.1
0.2
0.3
0.4
0.5
0.6
0.7
DISTANCE (mm) OUTSIDE OUTLET CROSS-SECTION

Figure 21

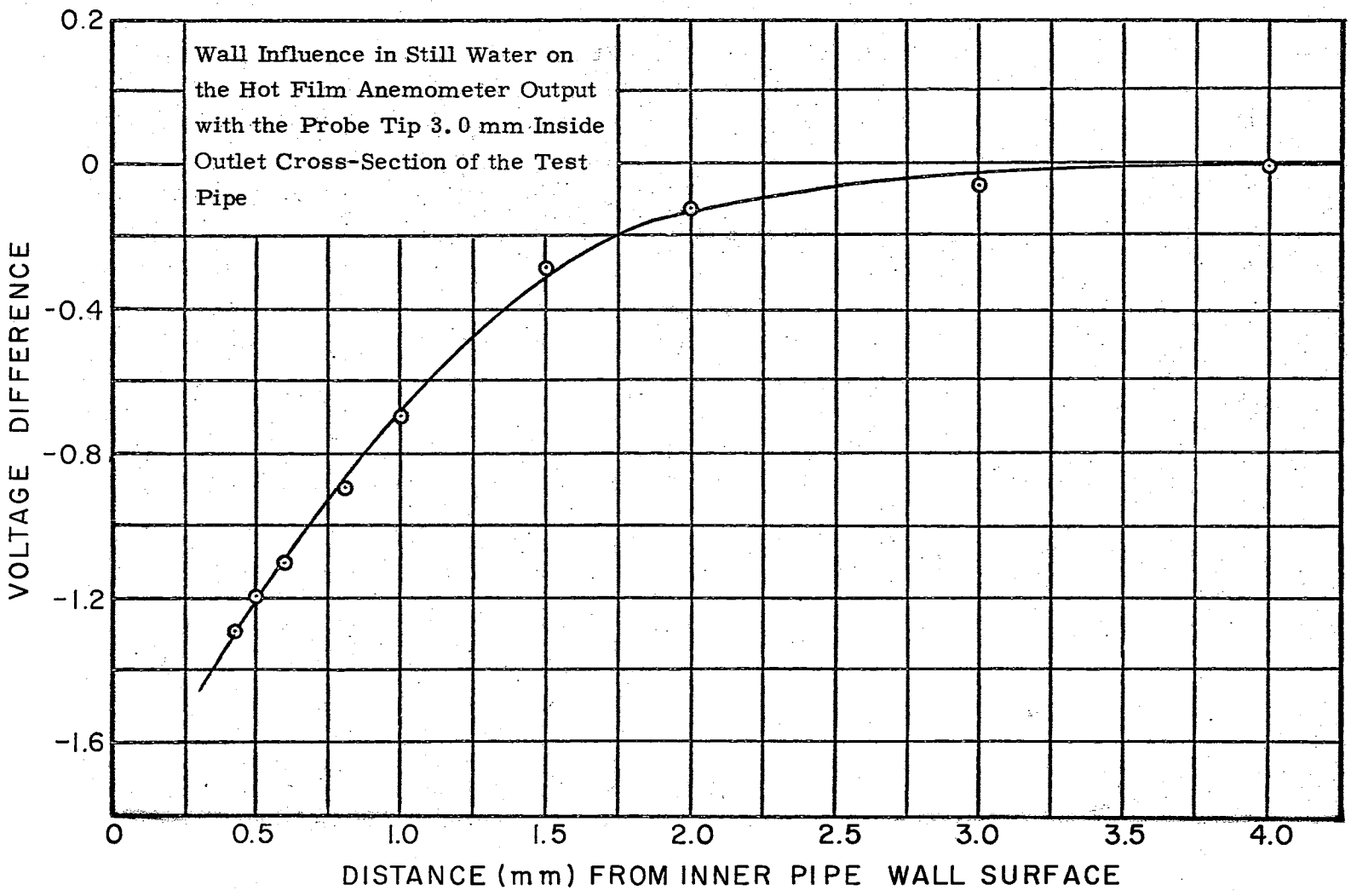
Wall Influence in Still Water on the Hot Film Anemometer Output with the Probe Tip 3.0 mm Inside Outlet Cross-Section of the Test Pipe
VOLTAGE DIFFERENCE
0.2
0
-0.4
-0.8
-1.2
-1.6
0
0.5
1.0
1.5
2.0
2.5
3.0
3.5
4.0
DISTANCE (mm) FROM INNER PIPE WALL SURFACE

Figure 22

the final velocity measurements for the four Reynold's number tests with a correction for the effect of the wall on the heat transfer characteristics in still water.

The results for the four tests in the core area are very similar to the previous tests 0.1 mm and 0.3 mm outside the outlet cross-section. The two high Reynold's number tests show a verification of the "Law of the Wall", and all tests indicate a logarithmic region between the core area and the inner region. However, contrary to the results outside the outlet cross-section the tests Re = 29,000 and Re = 46,200 indicated much lower values than the "Law of the Wall" predicts for velocities measured near the wall. These results agree with Laufer's results (6) for velocities near the wall in which he obtained unreasonably low values for velocities near the wall.

A rough correction for the effect of this probe on velocity measurements near the wall was attempted in a series of tests using the tow tank mechanism of Section 4.2.

The hot-film probe tip was positioned below a wall simulation device as illustrated in Figure 24 and towed through the distilled water at a constant velocity the same as described in Section 4.2. Figure 25 illustrates the results of these tests. The tests did not give conclusive or quantitative results, because the wall simulation device dragged water interfering with the hot-film results. In addition, this method could not possibly give a true simulation of the flow of water along the inner pipe wall. However, the test did indicate a definite trend of lower velocities near the wall owing to the presence of the probe.

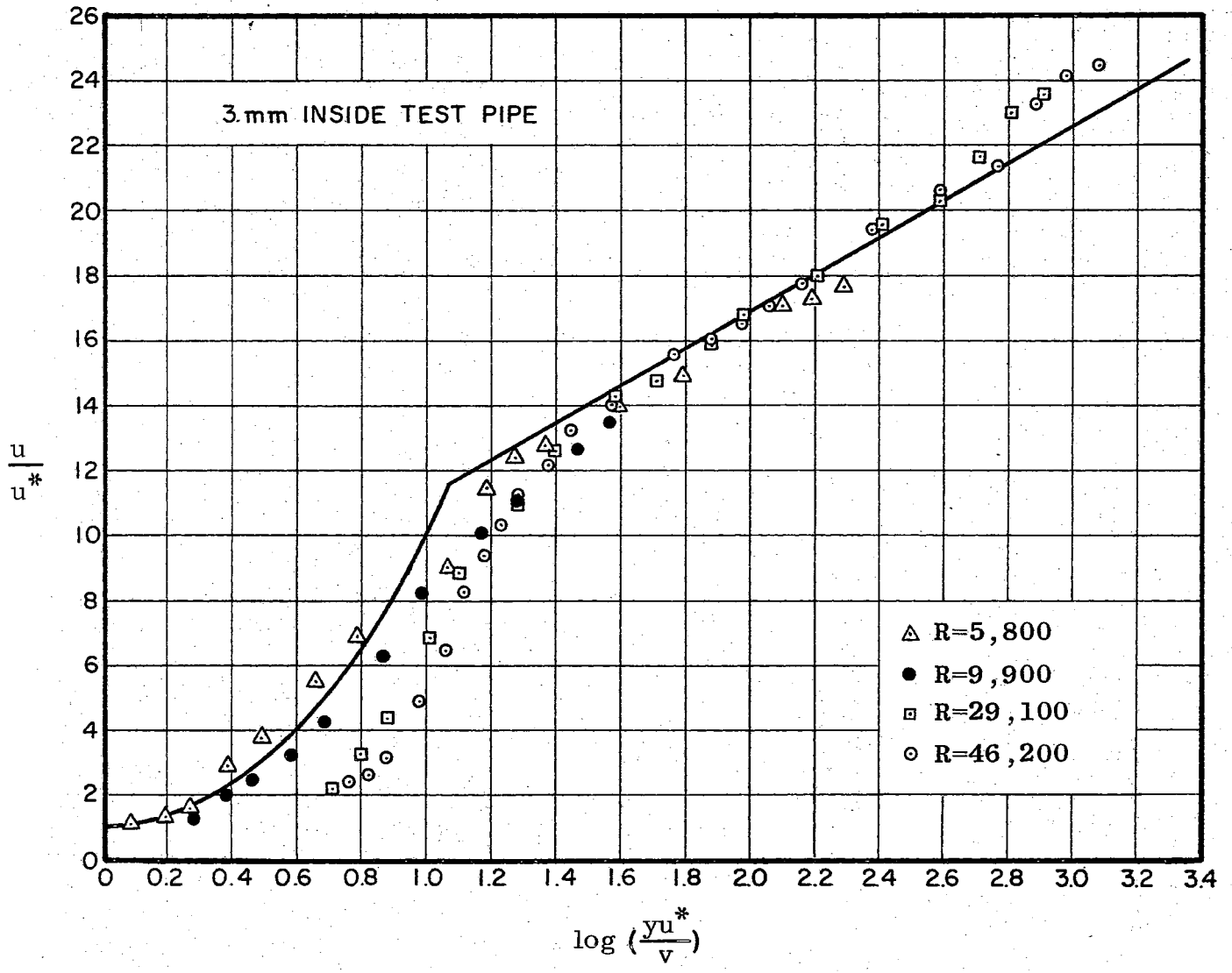
3.mm INSIDE TEST PIPE
R=5,800
R=9,900
R=29,100
R=46,200
u/u*
log (yu*/v)
0
2
4
6
8
10
12
14
16
18
20
22
24
26
0
0.2
0.4
0.6
0.8
1.0
1.2
1.4
1.6
1.8
2.0
2.2
2.4
2.6
2.8
3.0
3.2
3.4

Figure 23

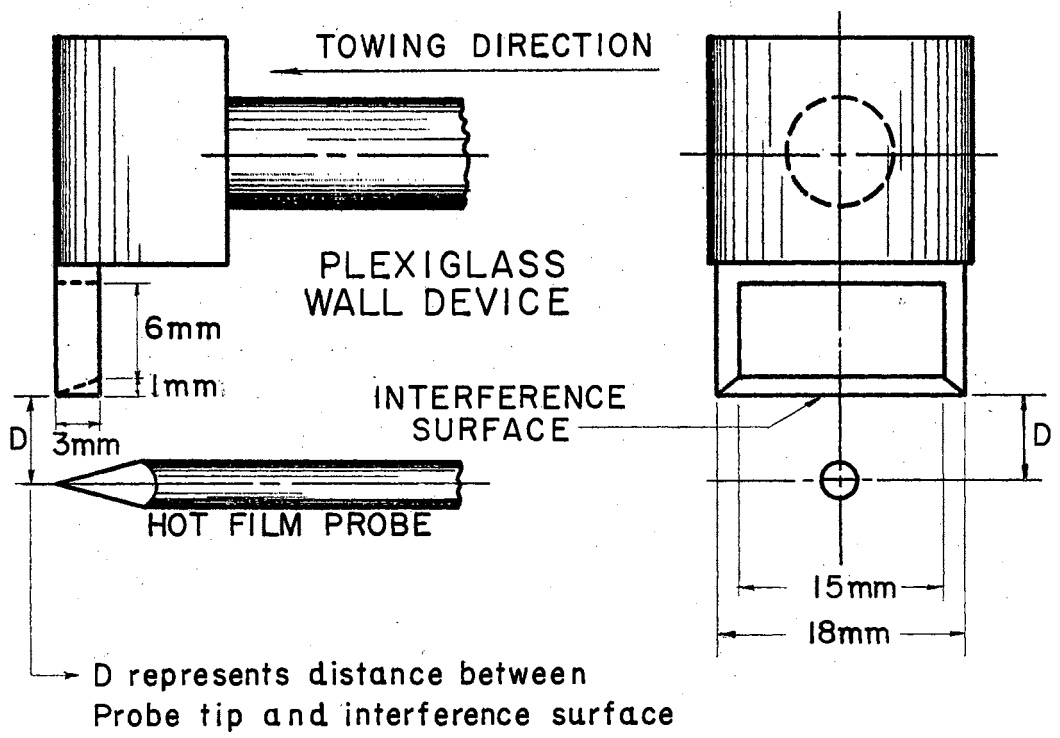
TOWING DIRECTION
PLEXIGLASS
WALL DEVICE
6mm
1mm
INTERFERENCE
SURFACE
D
3mm
HOT FILM PROBE
D
15mm
18mm
D represents distance between
Probe tip and interference surface

Figure 24

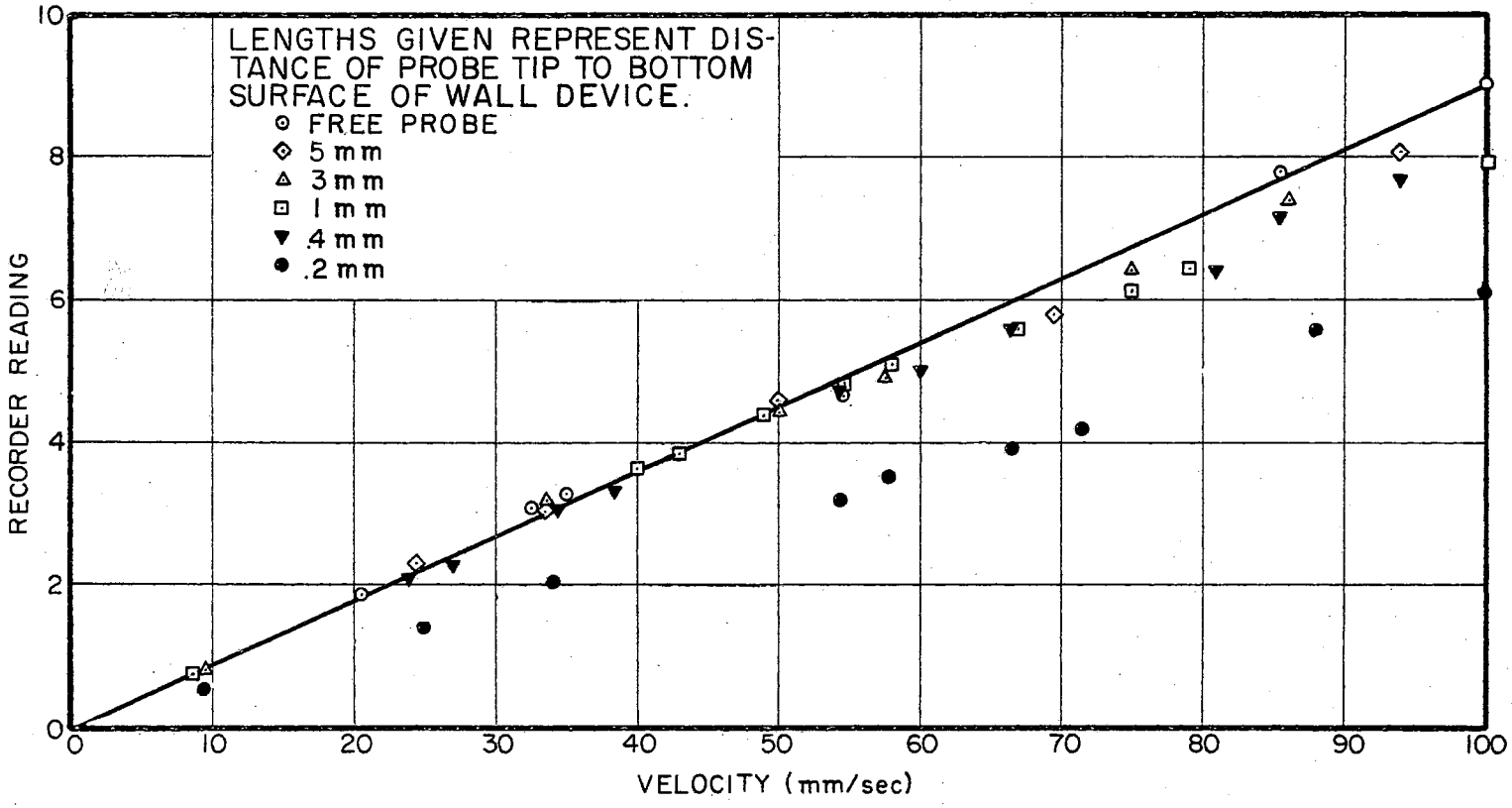
LENGTHS GIVEN REPRESENT DISTANCE OF PROBE TIP TO BOTTOM SURFACE OF WALL DEVICE.
FREE PROBE
5 mm
3 mm
1 mm
.4 mm
.2 mm
RECORDER READING
VELOCITY (mm/sec)
0
2
4
6
8
10
0
10
20
30
40
50
60
70
80
90
100

Figure 25

5.3. Results from Tests with a Canopy Situated on the Outlet of the Test Pipe

A canopy of dimensions and shape shown in Figure 26 was fastened to the end of the test pipe in a manner so the walls of the canopy were essentially a continuation of the test pipe wall. The canopy had a 3.2 mm slit machined in the top wall which permitted the probe tip to be raised behind the test pipe wall. It was anticipated: a) that the slit would allow measurements behind the test wall, but would eliminate the effect of the size of the probe itself on the velocity measurements as was present in the measurements of Section 5.2; b) that the presence of the canopy would essentially eliminate most jet dispersion effects which could have been present in the measurements of Section 5.1.

Before the tests with the canopy were run, another check on the change in the probe heat-transfer characteristics in still water near the wall was made with the canopy in place. Figure 27 shows this test. The correction for this effect was not significant compared to the actual velocities and was neglected in the results.

The results from the tests with the canopy are shown in Figure 28. Except for an extremely small deviation from the linear curve at distances less than 0.10 mm from the wall, the results are a confirmation of both the "Law of the Wall" and the "Law of the Wake". However, the straight line region, representing the logarithmic relationship between velocity and distance is slightly lower than Nikuradse's results. This effect was consistently noticeable in all of the tests.

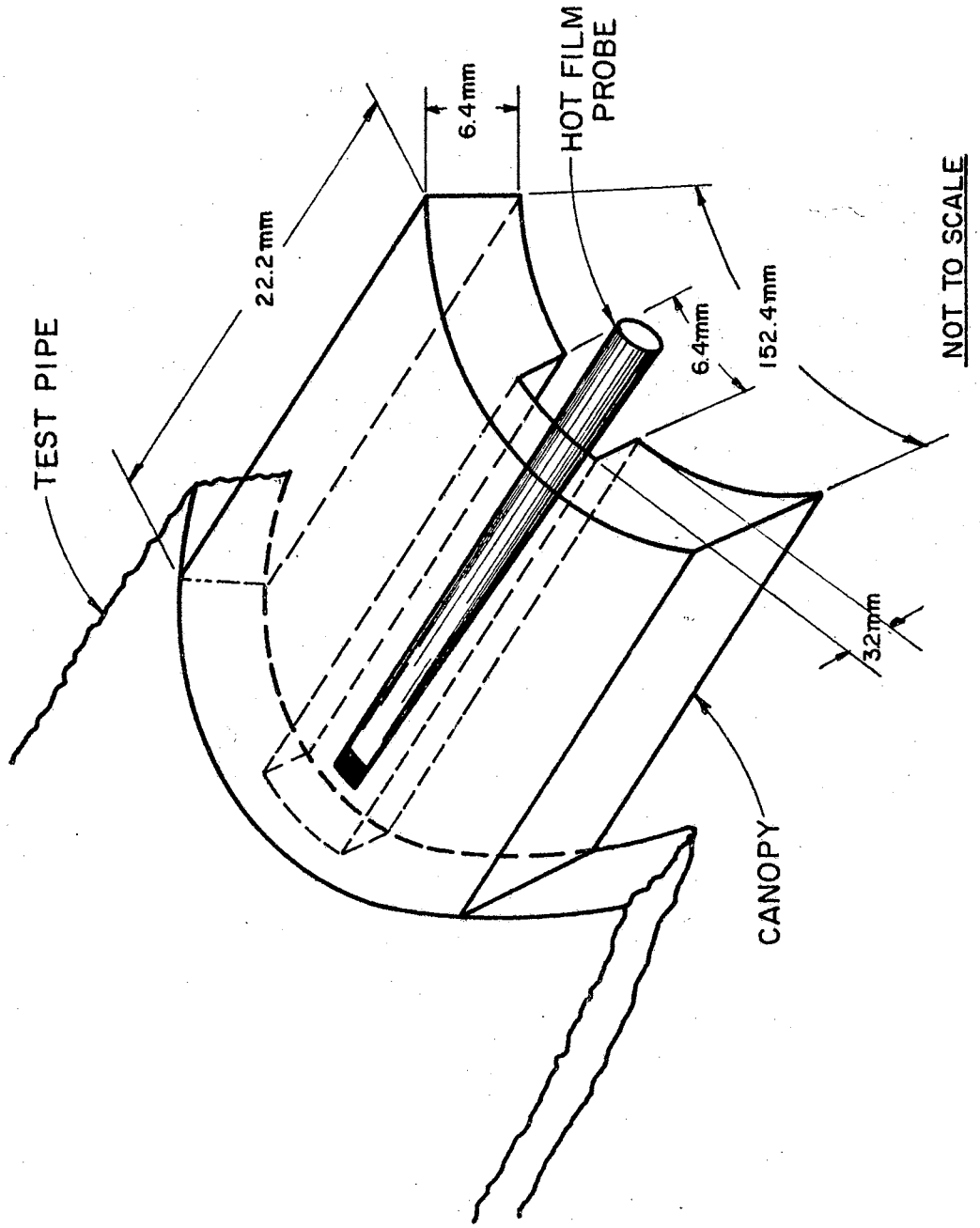
TEST PIPE
22.2mm
6.4mm
HOT FILM PROBE
6.4mm
152.4mm
NOT TO SCALE
32mm
CANOPY

Figure 26

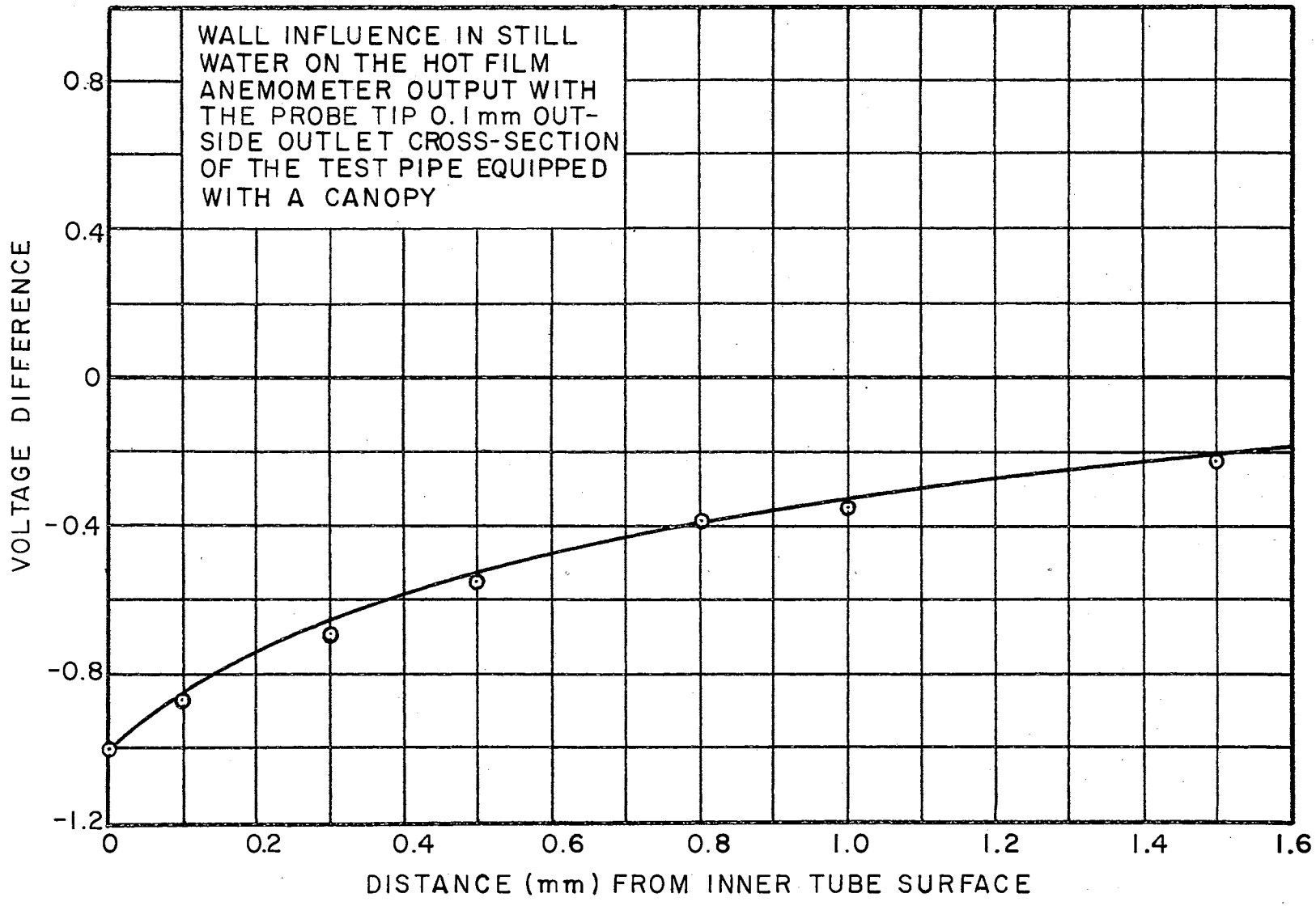
WALL INFLUENCE IN STILL WATER ON THE HOT FILM ANEMOMETER OUTPUT WITH THE PROBE TIP 0.1mm OUTSIDE OUTLET CROSS-SECTION OF THE TEST PIPE EQUIPPED WITH A CANOPY
VOLTAGE DIFFERENCE
0.8
0.4
0
-0.4
-0.8
-1.2
0
0.2
0.4
0.6
0.8
1.0
1.2
1.4
1.6
DISTANCE (mm) FROM INNER TUBE SURFACE

Figure 27

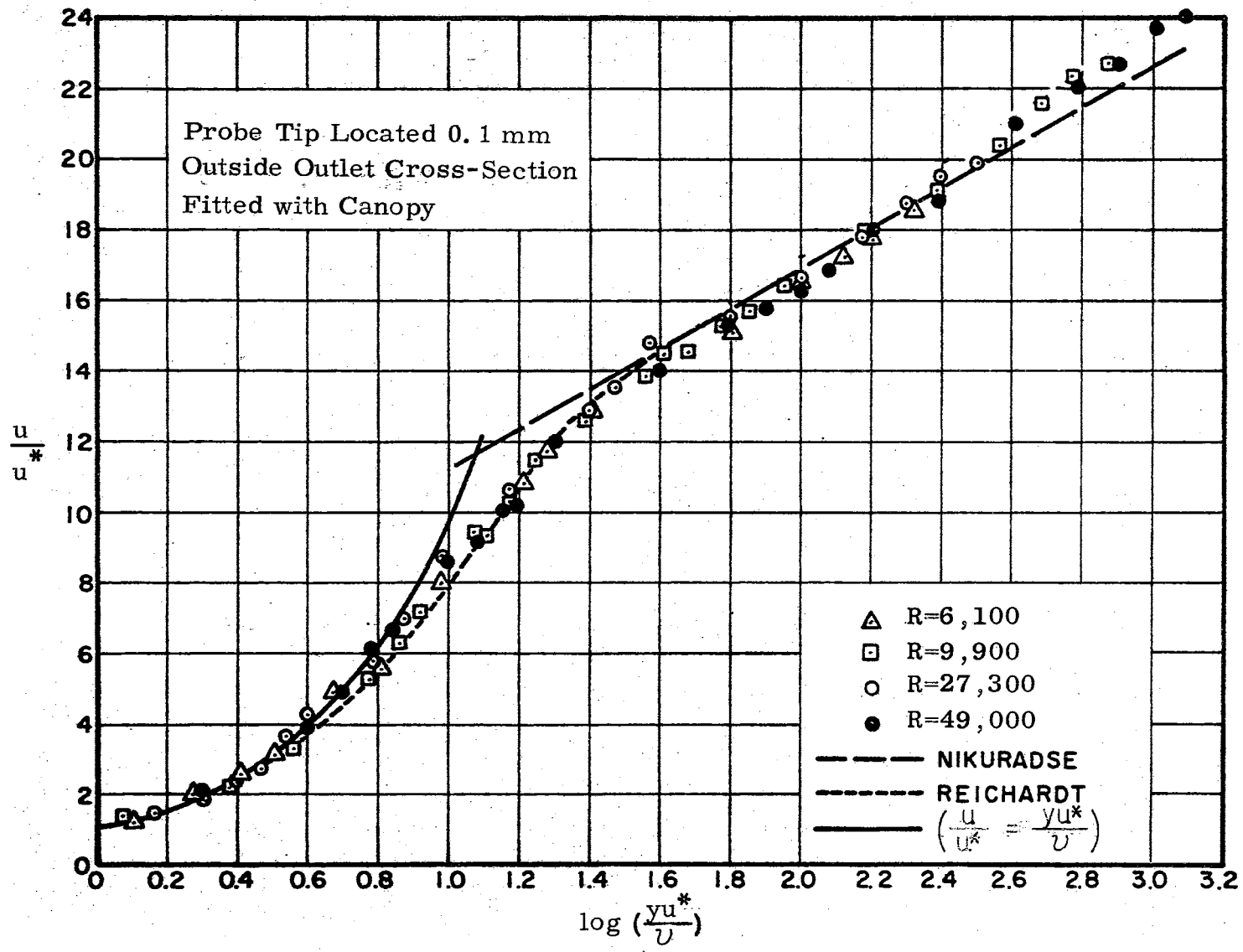
Probe Tip Located 0.1 mm
Outside Outlet Cross-Section
Fitted with Canopy
R=6,100
R=9,900
R=27,300
R=49,000
NIKURADSE
REICHARDT
$\left(\frac{u}{u^*} = \frac{yu^*}{\upsilon}\right)$
$\frac{u}{u^*}$
$\log\left(\frac{yu^*}{\upsilon}\right)$
0 2 4 6 8 10 12 14 16 18 20 22 24
0 0.2 0.4 0.6 0.8 1.0 1.2 1.4 1.6 1.8 2.0 2.2 2.4 2.6 2.8 3.0 3.2

Figure 28

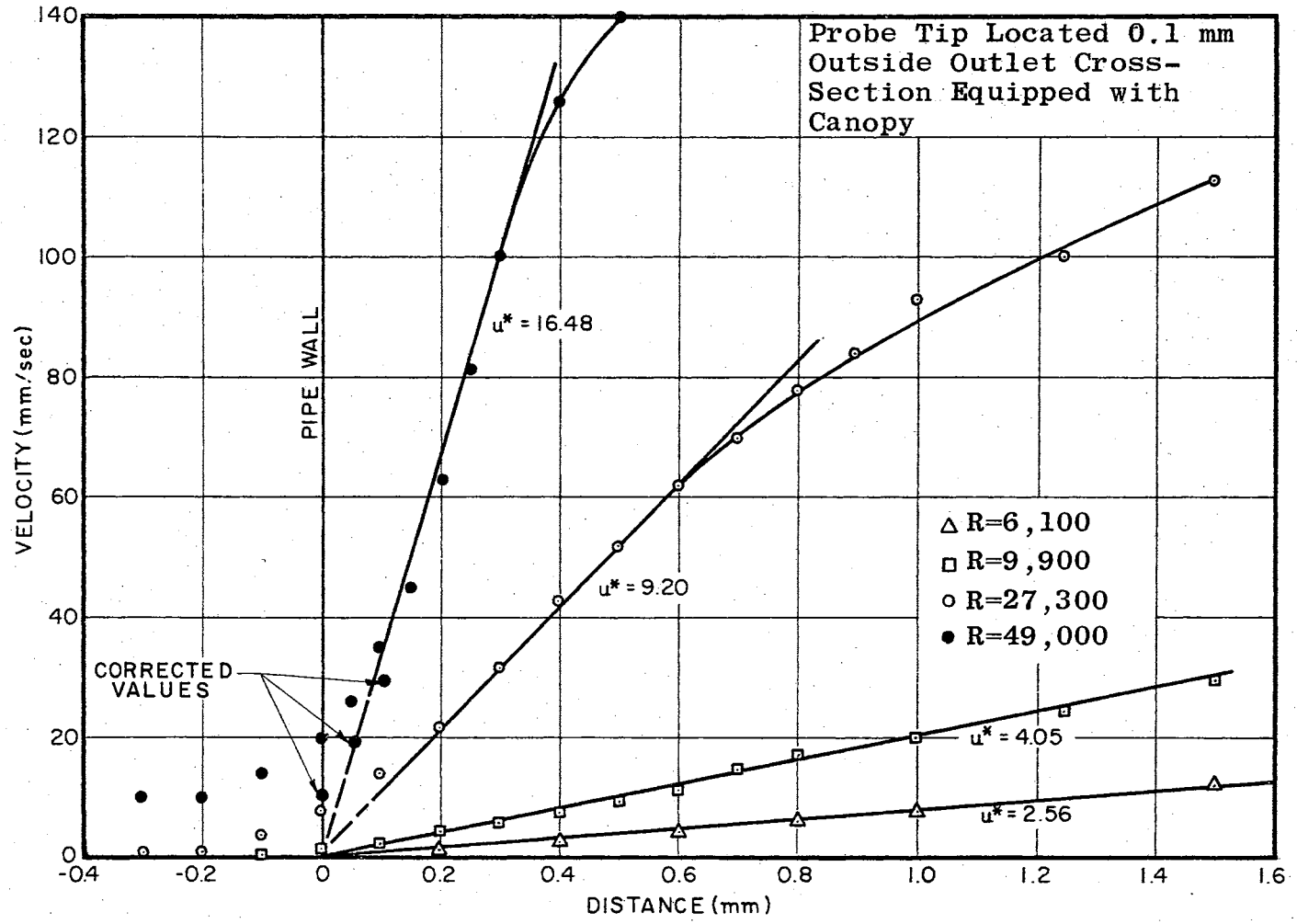
Probe Tip Located 0.1 mm Outside Outlet Cross-Section Equipped with Canopy
VELOCITY (mm/sec)
DISTANCE (mm)
PIPE WALL
u* = 16.48
u* = 9.20
u* = 4.05
u* = 2.56
CORRECTED VALUES
△ R=6,100
□ R=9,900
○ R=27,300
● R=49,000
140
120
100
80
60
40
20
0
-0.4
-0.2
0
0.2
0.4
0.6
0.8
1.0
1.2
1.4
1.6

Figure 29

Figure 29 shows the velocity measurements near the wall in detail. Again a finite velocity was measured at the position $y = 0$ for the high Reynold's number tests. This finite velocity at the position $y = 0$, and positions behind the wall could probably be attributed to secondary currents existing in the canopy slot. This, however, was the greatest source of uncertainty in this investigation. The order of magnitude of the finite velocity at $y = 0$ decreased sharply from the tests without the canopy to tests with the canopy, indicating a reduction in jet dispersion effects.

The change in velocity with the probe tip's distance from the outlet cross-section was investigated for the tests with the canopy. Figure 30 gives the results. Except for experimental scatter the results are identical.

5.4. Comparison of Wall Friction Velocities

A check on the accuracy of velocity measurements can be made from pipe friction calculations. Although the wall friction velocity u^* was not measured directly in this investigation, it can be calculated accurately from known empirical formulas which have been confirmed by numerous experimental investigations. The wall friction velocity u^* was calculated by using Blasius formula (see Section 2.2).

The friction velocity also can be determined from the measured velocity gradient at the wall. A comparison of these u^* values is shown in Figure 31. Very good agreement between the measured and calculated u^* values is indicated especially by using the corrected u^* values. The corrected u^* values were calculated from velocity gradients taken from plots of corrected velocities (see Figures 16, 18, 29).

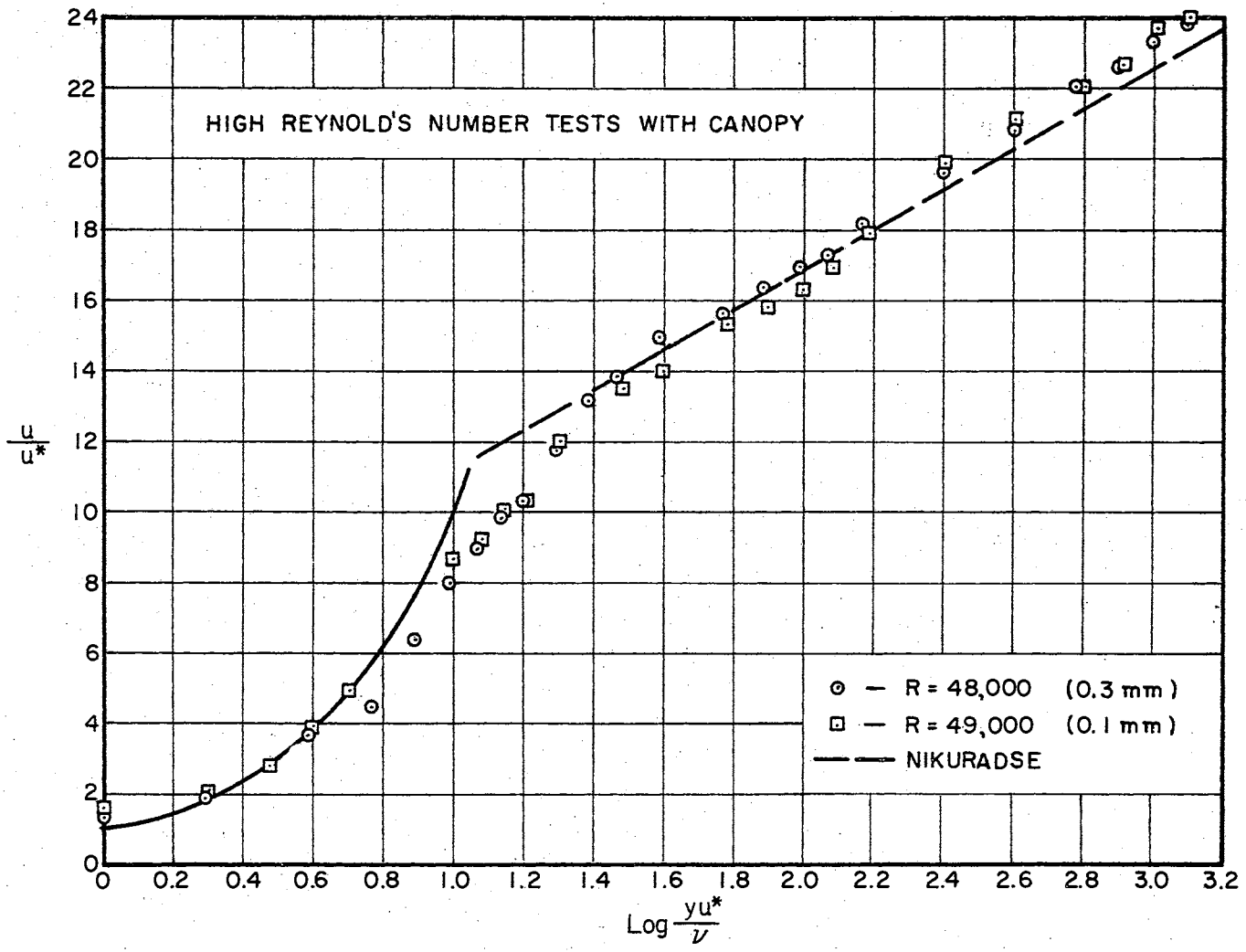
HIGH REYNOLD'S NUMBER TESTS WITH CANOPY
⊙ — R = 48,000 (0.3 mm)
⊡ — R = 49,000 (0.1 mm)
NIKURADSE
u/u*
Log yu*/ν
0
2
4
6
8
10
12
14
16
18
20
22
24
0
0.2
0.4
0.6
0.8
1.0
1.2
1.4
1.6
1.8
2.0
2.2
2.4
2.6
2.8
3.0
3.2

Figure 30

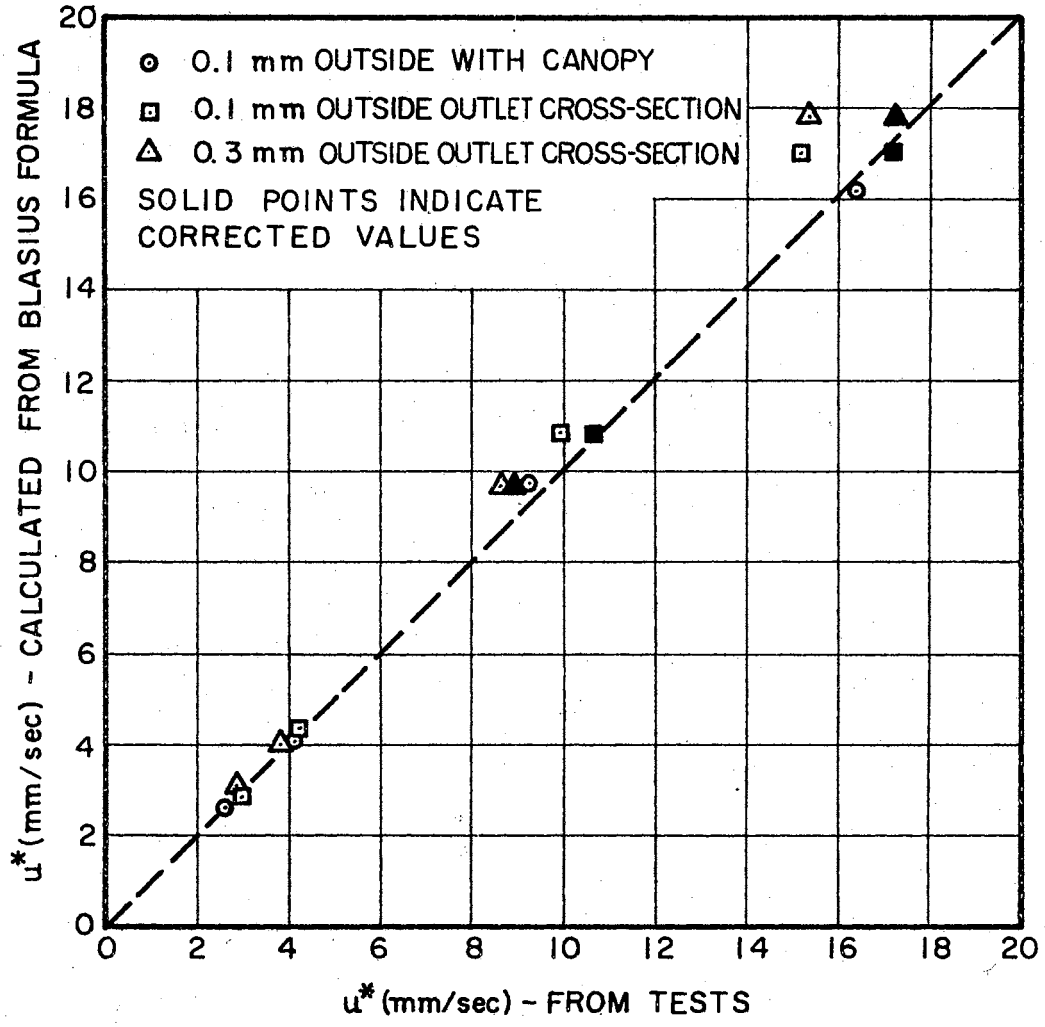
0.1 mm OUTSIDE WITH CANOPY
0.1 mm OUTSIDE OUTLET CROSS-SECTION
0.3 mm OUTSIDE OUTLET CROSS-SECTION
SOLID POINTS INDICATE
CORRECTED VALUES
u* (mm/sec) - CALCULATED FROM BLASIUS FORMULA
u* (mm/sec) - FROM TESTS
0
2
4
6
8
10
12
14
16
18
20

Figure 31

CHAPTER VI

SUMMARY

Three series of tests were conducted measuring the mean velocity distribtuion in fully developed turbulent flow of water in a straight pipe by the use of hot-film probe anemometer technique.

In the first series of tests, the probe tip was located outside the pipe outlet section. The results from these tests showed a confirmation of the "Law of the Wake" in the core area (a slightly different logarithmic relationship in the inner area than Nikuradse's reported results). A deviation from the usual viscous sublayer hypothesis (linear variation of velocity with distance) in the wall region was observed. A finite velocity was measured at the wall surface position and furthermore velocity persisted even with probe positions behind the wall. The horizontal distance of the probe tip to the outlet cross-section was varied and the subsequent change in velocity profile was measured. This change in velocity profile with horizontal distance of the probe tip to the outlet cross-section was confined almost entirely to the wall region. The velocity measured at the wall decreased sharply with decreasing distances to the outlet cross-section. A correction for "background velocity" was applied to the velocity results near the wall which decreased but did not bring the wall velocity to zero.

A second series of tests with the probe inserted 3 mm inside the pipe outlet section also gave results consistent with the mean

velocity hypothesis for the core area and was essentially the same as the results obtained from the first series of tests. However, contrasting with the high velocity deviations from the viscous sublayer hypothesis obtained with the probe tip outside the outlet near the wall, the velocity measured near the wall for the probe tip inserted inside the pipe gave velocities much lower than predicted by the viscous sublayer hypothesis. This deviation increased with increasing Reynold's number. A crude test was run with a wall device mounted above the probe tip attempting to substantiate the assumption that the relatively large size of the probe caused the deviations in the velocity measurements near the wall. This test indicated lower velocities measured with the wall device close to the probe tip than was present with a free probe, if both were towed through still water at the same towing rate.

Finally, the third series of tests with a canopy fitted to the pipe end showed confirmation of the present mean velocity hypothesis in all the pipe cross-section except for a very small distance (0.1 mm) away from the pipe wall. This deviation was probably due to the small secondary current which could exist in the canopy slot. The canopy was an effective way to eliminate most of the jet dispersion effects which were present in the first series of tests with the probe tip outside the outlet cross-section.

The problem stated in Chapter I now is resolved.

(1) Nikuradse's work reported in 1930 is in error both in his results for the region near the wall and the region in the core area.

(2) The "Law of the Wall" is shown valid as near as 0.1 mm from the pipe wall and it is concluded from the results of the test with the canopy that any deviation from the "Law of the Wall" is caused by the experimental technique used.

(3) There is a definite deviation from the logarithmic relationship in the core area which is in agreement with the "Law of the Wake" hypothesis.

BIBLIOGRAPHY

1. Stanton, Marshall and Bryant, "Conditions at the Boundary of a Fluid in Turbulent Motion," Proc. Roy. Soc. of London, p. 97, Vol. 413, 1920.

2. Nikuradse, J. "Widerstandsgesetz und Geschwindigkeit verteilung von turbulenten Wasserströmungen in glatten und rauhen Röhren." Proc. 3rd ICAM, Vol. I, p. 239, Stockholm, 1930.

3. Nikuradse, J. "Gesetzmässigkeiten der turbulenten Strömung in Glatten Rohren." Forschungs-Heft 356, Berlin, Germany, 1932.

4. Miller, Benjamin. "The Laminar Film Hypothesis." Trans. of the ASME, Vol. 71, No. 4, May, 1949, pp. 357-368.

5. Reichardt, H. "Die Warmuebertragung in flubulenten Reibungs-schichter." Zeitschrift für Angewandtle Mathematik und Mechanik. Vol. 20, 1940, pp. 297-328, translated in N.A.C.A. Tech. Memo. No. 1047, 1943.

6. Laufer, J. "The Structure of Turbulence in Fully Developed Pipe Flow," N.A.C.A. Report No. 1174, Oct. 28, 1952.

7. Schubauer, G. B. "Air Flow in a Separating Laminar Boundary Layer." N.A.C.A. Report No. 527, 1934.

8. Dryden, H. L. "Air Flow in the Boundary Layer near a Plate." N.A.C.A. Report No. 527, 1934.

9. Abbrect, P. and S. Churchill. "The Thermal Entrance Region in Fully Developed Turbulent Flow." A.I.Ch.E. Journal, Vol. 6, No. 2, pp. 268-273.

10. Nunner, W. Forschung a.d. Gebiete Ingenieur Wesen, Heft. No. 455, 1956.

11. Deissler, R. G. N.A.C.A. Tech. Note. 2138, 1950.

12. Rothfus, R. R., C. C. Monrad and V. E. Senecal. "Velocity Distribution and Fluid Friction in Smooth Concentric Annuli." Ind. and Eng. Chem. Vol. 42, No. 12, 1950.

13. Coles, D. "The Law of the Wake in Turbulent Boundary Layer." J. of Fluid Mech., Vol. 1, 1950.

14. Clauser, F. H. "The Turbulent Boundary Layer." Adv. in Applied Mech., Vol. IV, pp. 1-56, Academic Press, 1956.

15. Hinze, J. O. Turbulence. New York: McGraw-Hill Book Co., Inc., 4th Ed., 1962.

16. Prandl, L. "Über die ausgebildete Turbulenz Reibungsschichten." ZAMM 20, 297 (1940) also see N.A.C.A. TM 1047 (1943).

17. Von Karman, Th. "Mechanische Aehnlichkeit und Turbulenz," Nachr. Ges. Wiss. Goettingen, p. 68, 1930.

18. Millikan, C. B. "A Critical Discussion of Turbulent Flow in Channels and Circular Tubes," Proc. 5th Int. Cong. Applied Mech., Cambridge, pp. 386-392, 1938.

19. Ling, Sung-Ching. "Measurement of Flow Characteristics by the Hot-Film Technique," Ph. D. Dissertation, State Univerwity of Iowa, 1955.

20. Schlichting, D. Boundary Layer Theory. New York: McGraw-Hill Book Co., Inc., 4th Edition, 1962.

APPENDIX A - TEST RESULTS

TEST 21 DATE 4- 0-65 .3 mm inside

U*= 4.02 Q= 12.7 U= .818 R= 9859.

Y	NU	LOG(NU)	U	PHI
63.50	312.1	2.49	71.5	17.78
50.80	249.7	2.40	70.0	17.41
40.70	200.0	2.30	68.5	17.04
30.80	151.4	2.18	65.5	16.29
20.30	99.8	2.00	62.0	15.42
12.70	62.4	1.80	55.5	13.80
7.60	37.4	1.57	54.2	13.48
6.00	29.5	1.47	50.5	12.56
4.00	19.7	1.29	45.0	11.19
3.00	14.7	1.17	40.5	10.07
2.00	9.8	.99	32.8	8.16
1.50	7.4	.87	25.2	6.27
1.00	4.9	.69	16.8	4.18
.80	3.9	.59	13.0	3.23
.60	2.9	.47	10.0	2.49
.50	2.5	.39	8.0	1.99
.40	2.0	.29	5.3	1.32

TEST 23 DATE 4- 0-65 .3 mm inside

U*= 10.37 Q= 37.5 U= .818 R= 29111.

Y	NU	LOG(NU)	U	PHI
63.50	804.9	2.91	245.0	23.63
50.80	643.9	2.81	238.0	22.95
40.70	515.9	2.71	224.0	21.60
30.80	390.4	2.59	210.0	20.25
20.30	257.3	2.41	203.6	19.64
12.70	161.0	2.21	186.3	17.97
7.60	96.3	1.98	173.7	16.75
6.00	76.1	1.88	164.5	15.87
4.00	50.7	1.71	153.0	14.76
3.00	38.0	1.58	148.0	14.27
2.00	25.4	1.40	131.1	12.64
1.50	19.0	1.28	113.9	10.99
1.00	12.7	1.10	92.0	8.87
.80	10.1	1.01	71.3	6.88
.60	7.6	.88	46.0	4.44
.50	6.3	.80	34.5	3.33
.40	5.1	.71	23.0	2.22

TEST 14 DATE 3- 31-65 .3 mm outside

U*= 17.90 Q= 69.1 U= .894 R= 49081.

Y	NU	LOG(NU)	U	PHI
63.50	1271.3	3.10	462.8	25.86
50.80	1017.0	3.01	452.4	25.28
40.70	814.8	2.91	442.0	24.70
30.80	616.6	2.79	421.1	23.53
20.30	406.4	2.61	394.0	22.01
12.70	254.3	2.41	358.0	20.00
7.60	152.1	2.18	322.5	18.02
6.00	120.1	2.08	318.0	17.77
5.00	100.1	2.00	306.0	17.10
4.00	80.1	1.90	293.0	16.37
3.00	60.1	1.78	276.0	15.42
2.00	40.0	1.60	262.0	14.64
1.50	30.0	1.48	247.0	13.80
1.00	20.0	1.30	224.0	12.52
.80	16.0	1.20	212.0	11.85
.60	12.0	1.08	189.0	10.56
.50	10.0	1.00	176.0	9.83
.40	8.0	.90	153.0	8.55
.30	6.0	.78	133.0	7.43
.20	4.0	.60	105.0	5.87
.10	2.0	.30	77.0	4.30
.05	1.0	.00	66.0	3.69
.00	.0	.00	53.0	2.96

TEST 28 DATE 4- 0-65 .3 mm inside

U*= 15.53 Q= 59.5 U= .818 R= 46189.

Y	NU	LOG(NU)	U	PHI
63.50	1205.5	3.08	380.0	24.47
50.80	964.4	2.98	375.0	24.15
40.70	772.6	2.89	360.0	23.18
30.80	584.7	2.77	333.0	21.44
20.30	385.4	2.59	321.0	20.67
12.70	241.1	2.38	302.0	19.45
7.60	144.3	2.16	277.0	17.84
6.00	113.9	2.06	265.0	17.07
5.00	94.9	1.98	258.0	16.61
4.00	75.9	1.88	250.0	16.10
3.00	57.0	1.76	242.0	15.58
2.00	38.0	1.58	218.0	14.04
1.50	28.5	1.45	206.0	13.27
1.25	23.7	1.38	190.0	12.24
1.00	19.0	1.28	175.0	11.27
.90	17.1	1.23	160.0	10.30
.80	15.2	1.18	146.0	9.40
.70	13.3	1.12	129.0	8.31
.60	11.4	1.06	101.0	6.50
.50	9.5	.98	76.0	4.89
.40	7.6	.88	50.0	3.22
.35	6.6	.82	40.0	2.58
.30	5.7	.76	37.0	2.38

TEST 12 DATE 3- 28-65 .3 mm outside

U*= 4.07 Q= 12.7 U= .877 R= 9232.

Y	NU	LOG(NU)	U	PHI
63.50	294.6	2.47	78.0	19.17
50.80	235.7	2.37	76.0	18.68
40.70	188.9	2.28	73.5	18.06
30.80	142.9	2.16	70.0	17.20
20.30	94.2	1.97	68.0	16.71
12.70	58.9	1.77	63.0	15.48
7.60	35.3	1.55	59.0	14.50
6.00	27.8	1.44	56.0	13.76
4.00	18.6	1.27	50.0	12.29
2.00	9.3	.97	37.0	9.09
1.50	7.0	.84	27.5	6.76
1.00	4.6	.67	22.0	5.41
.75	3.5	.54	18.0	4.42
.50	2.3	.37	12.5	3.07
.25	1.2	.06	7.0	1.72

TEST 13 DATE 3- 28-65 .3 mm outside

U*= 2.52 Q= 7.4 U= .858 R= 5477.

Y	NU	LOG(NU)	U	PHI
63.50	186.6	2.27	46.0	18.25
50.80	149.3	2.17	44.0	17.45
40.70	119.6	2.08	42.5	16.86
30.80	90.5	1.96	40.0	15.87
20.30	59.6	1.78	37.5	14.87
12.70	37.3	1.57	33.5	13.29
7.60	22.3	1.35	32.5	12.89
6.00	17.6	1.25	29.5	11.70
4.00	11.8	1.07	24.5	9.72
2.00	5.9	.77	16.0	6.35
1.50	4.4	.64	13.0	5.16
1.00	2.9	.47	8.5	3.37
.75	2.2	.34	5.8	2.30
.50	1.5	.17	4.5	1.78
.25	.7	-.12	3.0	1.19
.00	.0	.00	1.5	.59

TEST 11 DATE 3- 28-65 .3 mm outside

U*= 9.79 Q= 34.8 U= .871 R= 25371.

Y	NU	LOG(NU)	U	PHI
63.50	713.6	2.85	219.0	22.37
50.80	570.9	2.76	213.0	21.76
40.70	457.4	2.66	208.0	21.25
30.80	346.1	2.54	200.0	20.43
20.30	228.1	2.36	188.5	19.26
12.70	142.7	2.15	176.5	18.03
7.60	85.4	1.93	162.0	16.55
6.00	67.4	1.83	156.3	15.97
4.00	45.0	1.65	145.5	14.86
2.00	22.5	1.35	122.6	12.52
1.50	16.9	1.23	114.6	11.71
1.00	11.2	1.05	99.5	10.16
.70	7.9	.90	75.0	7.66
.40	4.5	.65	58.0	5.93
.25	2.8	.45	39.5	4.04
.10	1.1	.05	25.3	2.58
.00	.0	.00	19.5	1.99

TEST 29 DATE 4- 12-65 .3 mm outside

U*= 2.80 Q= 8.3 U= .897 R= 5876.

Y	NU	LOG(NU)	U	PHI
63.50	198.4	2.30	52.0	18.55
50.80	158.7	2.20	51.0	18.19
40.70	127.2	2.10	49.5	17.66
30.80	96.2	1.98	47.5	16.95
20.30	63.4	1.80	45.5	16.23
12.70	39.7	1.60	41.0	14.63
7.60	23.7	1.38	38.5	13.74
6.00	18.7	1.27	35.5	12.66
5.00	15.6	1.19	34.0	12.13
4.00	12.5	1.10	30.5	10.88
3.00	9.4	.97	26.0	9.28
2.00	6.2	.80	20.5	7.31
1.00	3.1	.49	11.0	3.92
.80	2.5	.40	9.0	3.21
.60	1.9	.27	6.0	2.14
.40	1.2	.10	4.0	1.43
.20	.6	-.19	3.0	1.07
.10	.3	-.50	2.0	.71
.00	.0	.00	1.0	.36

TEST 30 DATE 4- 12-65 .3 mm outside

U*= 4.42 Q= 14.0 U= .881 R= 10091.

Y	NU	LOG(NU)	U	PHI
63.50	318.5	2.50	87.5	19.80
50.80	254.8	2.41	86.0	19.46
40.70	204.1	2.31	82.5	18.67
30.80	154.5	2.19	78.5	17.76
20.30	101.8	2.01	73.5	16.63
12.70	63.7	1.80	70.0	15.84
7.60	38.1	1.58	66.5	15.05
6.00	30.1	1.48	61.5	13.92
5.00	25.1	1.40	61.0	13.80
4.00	20.1	1.30	57.0	12.90
3.00	15.0	1.18	49.5	11.20
2.00	10.0	1.00	41.0	9.28
1.50	7.5	.88	34.5	7.81
1.00	5.0	.70	25.0	5.66
.80	4.0	.60	20.5	4.64
.60	3.0	.48	15.5	3.51
.40	2.0	.30	12.0	2.72
.20	1.0	.00	7.0	1.58
.10	.5	-.29	4.5	1.02
.00	.0	.00	3.5	.79

TEST 32 DATE 4- 12-65 .1 mm outside

U*= 17.01 Q= 65.5 U= .867 R= 47973.

Y	NU	LOG(NU)	U	PHI
63.50	1246.1	3.10	412.0	24.22
50.80	996.9	3.00	407.0	23.92
40.70	798.7	2.90	399.0	23.45
30.80	604.4	2.78	388.0	22.81
20.30	398.4	2.60	364.0	21.39
12.70	249.2	2.40	340.0	19.98
7.60	149.1	2.17	320.0	18.81
6.00	117.7	2.07	315.0	18.51
5.00	98.1	1.99	312.0	18.34
4.00	78.5	1.89	301.0	17.69
3.00	58.9	1.77	295.0	17.34
2.00	39.2	1.59	280.0	16.46
1.50	29.4	1.47	258.0	15.16
1.25	24.5	1.39	248.0	14.58
1.00	19.6	1.29	232.0	13.64
.80	15.7	1.20	210.0	12.34
.60	11.8	1.07	180.0	10.58
.40	7.8	.89	143.0	8.41
.30	5.9	.77	117.0	6.88
.20	3.9	.59	84.0	4.94
.10	2.0	.29	58.0	3.41
.05	1.0	-.00	45.0	2.64
.00	.0	.00	38.0	2.23
-.10	.0	.00	27.0	1.59
-.20	.0	.00	22.0	1.29
-.30	.0	.00	22.0	1.29

TEST 31 DATE 4- 12-65 .1 mm outside

U*= 10.77 Q= 38.7 U= .887 R= 27705.

Y	NU	LOG(NU)	U	PHI
63.50	770.8	2.89	242.0	22.48
50.80	616.6	2.79	238.0	22.11
40.70	494.0	2.69	230.0	21.36
30.80	373.9	2.57	216.0	20.06
20.30	246.4	2.39	201.0	18.67
12.70	154.2	2.19	188.0	17.46
7.60	92.2	1.96	180.0	16.72
6.00	72.8	1.86	169.0	15.70
5.00	60.7	1.78	160.0	14.86
4.00	48.6	1.69	158.0	14.68
3.00	36.4	1.56	152.0	14.12
2.00	24.3	1.39	137.0	12.72
1.50	18.2	1.26	124.0	11.52
1.00	12.1	1.08	106.0	9.85
.80	9.7	.99	91.0	8.45
.60	7.3	.86	80.0	7.43
.40	4.9	.69	56.0	5.20
.30	3.6	.56	46.0	4.27
.20	2.4	.39	32.0	2.97
.10	1.2	.08	20.0	1.86
.05	.6	-.21	15.0	1.39
.00	.0	.00	12.0	1.11
-.10	.0	.00	8.0	.74
-.20	.0	.00	6.5	.60
-.30	.0	.00	5.0	.46
-.40	.0	.00	5.0	.46

TEST 77 DATE 5- 17-65 .3 mm outside w/canopy

U*= 15.58 Q= 60.0 U= .794 R= 47985.

Y	NU	LOG(NU)	U	PHI
63.50	1246.4	3.10	373.0	23.93
50.80	997.1	3.00	364.0	23.36
40.70	798.9	2.90	354.0	22.71
30.80	604.5	2.78	344.0	22.07
20.30	398.4	2.60	326.0	20.92
12.70	249.3	2.40	305.0	19.57
7.60	149.2	2.17	284.0	18.22
6.00	117.8	2.07	270.0	17.32
5.00	98.1	1.99	265.0	17.00
4.00	78.5	1.89	255.0	16.36
3.00	58.9	1.77	244.0	15.66
2.00	39.3	1.59	234.0	15.01
1.50	29.4	1.47	216.0	13.86
1.25	24.5	1.39	206.0	13.22
1.00	19.6	1.29	184.0	11.81
.80	15.7	1.20	160.0	10.27
.70	13.7	1.14	154.0	9.88
.60	11.8	1.07	140.0	8.98
.50	9.8	.99	124.0	7.96
.40	7.9	.89	100.0	6.42
.30	5.9	.77	70.0	4.49
.20	3.9	.59	58.0	3.72
.10	2.0	.29	30.0	1.92
.00	.0	.00	21.0	1.35
-.10	.0	.00	10.0	.64
-.15	.0	.00	8.5	.55

TEST 72 DATE 5- 15-65 .1 mm outside w/canopy

U*= 4.05 Q= 12.8 U= .821 R= 9900.

Y	NU	LOG(NU)	U	PHI
63.50	313.2	2.50	80.5	19.88
50.80	250.6	2.40	79.0	19.51
40.70	200.8	2.30	76.0	18.77
30.80	151.9	2.18	72.0	17.78
20.30	100.1	2.00	67.5	16.67
12.70	62.6	1.80	63.0	15.56
7.60	37.5	1.57	59.0	14.57
6.00	29.6	1.47	55.0	13.58
5.00	24.7	1.39	52.5	12.96
4.00	19.7	1.30	49.5	12.22
3.00	14.8	1.17	43.0	10.62
2.00	9.9	.99	36.0	8.89
1.50	7.4	.87	29.0	7.16
1.25	6.2	.79	23.5	5.80
1.00	4.9	.69	20.0	4.94
.80	3.9	.60	17.5	4.32
.70	3.5	.54	15.0	3.70
.60	3.0	.47	11.5	2.84
.50	2.5	.39	9.5	2.35
.40	2.0	.30	7.5	1.85
.30	1.5	.17	6.0	1.48
.20	1.0	-.00	4.5	1.11
.10	.5	-.30	2.5	.62
.00	.0	.00	1.5	.37
-.10	.0	.00	.5	.12
-.20	.0	.00	.5	.12

U*= 9.78 Q= 35.1 U= .817 R= 27281. .1 mm outside w/canopy

Y	NU	LOG(NU)	U	PHI
63.50	760,4	2.88	222.0	22.69
50.80	608.3	2.78	219.0	22.38
40.70	487.4	2.69	211.0	21.57
30.80	368.8	2.57	200.0	20.44
20.30	243.1	2.39	187.0	19.11
12.70	152.1	2.18	175.0	17.89
7.60	91.0	1.96	160.0	16.35
6.00	71.9	1.86	154.0	15.74
5.00	59.9	1.78	150.0	15.33
4.00	47.9	1.68	143.0	14.62
3.00	35.9	1.56	136.0	13.90
2.00	24.0	1.38	123.0	12.57
1.50	18.0	1.25	113.0	11.55
1.25	15.0	1.18	101.0	10.32
1.00	12.0	1.08	93.0	9.51
.90	10.8	1.03	84.0	8.59
.80	9.6	.98	78.0	7.97
.70	8.4	.92	70.0	7.15
.60	7.2	.86	62.0	6.34
.50	6.0	.78	52.0	5.31
.40	4.8	.68	43.0	4.40
.30	3.6	.56	32.0	3.27
.20	2.4	.38	22.0	2.25
.10	1.2	.08	14.0	1.43
.00	.0	.00	8.0	.82
-.10	.0	.00	4.0	.41
-.20	.0	.00	1.0	.10
-.30	.0	.00	1.0	.10

TEST 75 DATE 5- 16-65 .1 mm outside w/canopy

U*= 16.19 Q= 62.5 U= .810 R= 48997.

Y	NU	LOG(NU)	U	PHI
63.5	1269.3	3.10	388.0	23.96
50.8	1015.5	3.01	384.0	23.72
40.7	813.6	2.91	368.0	22.73
30.8	615.7	2.79	357.0	22.05
20.3	405.8	2.61	340.0	21.00
12.7	253.9	2.40	306.0	18.90
7.6	151.9	2.18	290.0	17.91
6.0	119.9	2.08	274.0	16.92
5.0	99.9	2.00	264.0	16.30
4.0	80.0	1.90	256.0	15.81
3.0	60.0	1.78	247.0	15.25
2.0	40.0	1.60	227.0	14.02
1.5	30.0	1.48	218.0	13.46
1.0	20.0	1.30	194.0	11.98
.8	16.0	1.20	167.0	10.31
.7	14.0	1.15	164.0	10.13
.6	12.0	1.08	150.0	9.26
.5	10.0	1.00	140.0	8.65
.3	7.0	.84	126.0	7.78
.3	6.0	.78	100.0	6.18
.2	5.0	.70	81.0	5.00
.2	4.0	.60	63.0	3.89
.1	3.0	.48	45.0	2.78
.1	2.0	.30	35.0	2.16
.0	1.0	.00	26.0	1.61
.0	.0	.00	20.0	1.24

TEST 76 DATE 5- 16-65 .1 mm outside w/canopy

U*= 2.62 Q= 7.8 U= .817 R= 6062.

Y	NU	LOG(NU)	U	PHI
63.50	203.9	2.31	49.0	18.67
50.80	163.1	2.21	46.5	17.72
40.70	130.7	2.12	45.0	17.15
30.80	98.9	2.00	43.0	16.39
20.30	65.2	1.81	39.5	15.05
12.70	40.8	1.61	38.0	14.48
7.60	24.4	1.39	34.0	12.96
6.00	19.3	1.28	31.0	11.81
5.00	16.1	1.21	28.5	10.86
4.00	12.8	1.11	24.5	9.34
3.00	9.6	.98	21.0	8.00
2.00	6.4	.81	14.5	5.53
1.50	4.8	.68	13.0	4.95
1.00	3.2	.51	8.5	3.24
.80	2.6	.41	7.0	2.67
.60	1.9	.28	5.5	2.10
.40	1.3	.11	3.5	1.33
.20	.6	-.18	2.0	.76

VITA

Donald Frank Haber

Candidate for the Degree of

Doctor of Philosophy

Thesis: THE MEAN VELOCITY DISTRIBUTION IN FULLY DEVELOPED TURBULENT WATER FLOW IN STRAIGHT CIRCULAR PIPE

Major Field: Engineering

Biographical:

Personal Data: Born in St. Louis, Missouri, November 8, 1933, son of Frank L. Haber and Olga Haber.

Education: Attended elementary and secondary school in St. Louis, Missouri; graduated from Lutheran High School in 1951; Received the Bachelor of Science and Master of Science degrees from the University of Missouri at Rolla, with a major in Mining Engineering, in June 1956 and June 1962, respectively; attended National Science Summer Institutes for Engineering Teachers in 1961 and 1962 at Illinois Institute of Technology and Oklahoma State University, respectively; completed requirements for the degree of Doctor of Philosoply in May 1966.

Professional Experience: Employed with Carter Oil Company as a geophysicist from 1956 to 1957. Employed by McDonnell Aircraft, St. Louis, Missouri, as Associate Engineer 1957-1958; employed by the University of Missouri at Rolla from 1958 to 1962 as Instructor and Assistant Professor of Applied Mechanics; consultant with U.S. Bureau of Mines 1958-1961; recipient of a Ford Foundation Forgiveable Loan and employed part-time as Instructor of Civil Engineering at Oklahoma State University from September 1962 to January 1965. Employed with U.S. Department of the Interior as project superintendent, summers 1961, 1965. Employed as Instructor full-time with Oklahoma State University, September 1965 to present.